Acta Biomaterialia 156 (2023) 250–268

Contents lists available at ScienceDirect

Acta Biomaterialia

journal homepage: www.elsevier.com/locate/actbio

Review article

Biofabricating the vascular tree in engineered bone tissue☆

Leanne de Silva[a,b,*], Paulina N. Bernal[b,c], AJW Rosenberg[a], Jos Malda[b,c,d], Riccardo Levato[b,c,d], Debby Gawlitta[a,b,1]

[a] Department of Oral and Maxillofacial Surgery & Special Dental Care, University Medical Center Utrecht, Utrecht University, Utrecht, 3508 GA, the Netherlands
[b] Regenerative Medicine Center Utrecht, Utrecht, 3584 CT, the Netherlands
[c] Department of Orthopaedics, University Medical Center Utrecht, Utrecht University, Utrecht, 3508 GA, the Netherlands
[d] Department of Clinical Sciences, Faculty of Veterinary Medicine, Utrecht University, Utrecht, 3584 CT, the Netherlands

ARTICLE INFO

Article history:
Received 28 April 2022
Revised 22 August 2022
Accepted 23 August 2022
Available online 28 August 2022

Keywords:
Biofabrication
Vascularization
Tissue engineering
Bone tissue engineering

ABSTRACT

The development of tissue engineering strategies for treatment of large bone defects has become increasingly relevant, given the growing demand for bone substitutes. Native bone is composed of a dense vascular network necessary for the regulation of bone development, regeneration and homeostasis. A major obstacle in fabricating living, clinically relevant-sized bone mimics (1-10 cm^3) is the limited supply of nutrients, including oxygen to the core of the construct. Therefore, strategies to support vascularization are pivotal for the development of tissue engineered bone constructs. Creating a functional bone construct integrated with a vascular network, capable of delivering the necessary nutrients for optimal tissue development is imperative for translation into the clinics. The vascular system is composed of a complex network that runs throughout the body in a tree-like hierarchical branching fashion. A significant challenge for tissue engineering approaches lies in mimicking the intricate, multi-scale structures consisting of larger vessels (macro-vessels) which interconnect with multiple sprouting vessels (microvessels) in a closed network. The advent of biofabrication has enabled complex, out of plane channels to be generated and has laid the groundwork for the creation of multi-scale vasculature in recent years. This review highlights the key state-of-the-art achievements for the development of vascular networks of varying scales in the field of biofabrication with a particular focus for its application in developing a functional tissue engineered bone construct.

Statement of significance

There is a growing need for bone substitutes to overcome the limited supply of patient-derived bone. Bone tissue engineering aims to overcome this by combining stem cells with scaffolds to restore missing bone. The current bottleneck in upscaling is the lack of an integrated vascular network, required for the delivery of nutrients to cells. 3D bioprinting techniques has enabled the creation of complex hollow structures of varying dimensions that resemble native blood vessels. The convergence of multiple materials, cell types and fabrication approaches, opens the possibility of developing clinically-relevant sized vascularized bone constructs. This review provides an up-to-date insight of the technologies currently available for the generation of complex vascular networks, with a focus on their application in bone tissue engineering.

1. Introduction

Over the years, autologous bone has remained the “gold standard” replacement to restore large bone defects due to its inherent osteoinductive, osteoconductive and osteogenic properties [1]. Despite the fact that bone grafting techniques have become well-established and practiced over the past century, large bone defects

☆ Part of the Special Issue on Biofabrication for Orthopedic, Maxillofacial, and Dental Applications, guest-edited by Professors Hala Zreiqat, Khoon Lim, and Debby Gawlitta.

* Corresponding author at: Department of Oral and Maxillofacial Surgery & Special Dental Care, University Medical Center Utrecht, Utrecht University, G05.222, PO Box 85500, Utrecht, 3508 GA, the Netherlands.
E-mail address: L.S.deSilva@umcutrecht.nl (L. de Silva).

[1] Guest editors did not participate in, or have access to, the peer-review process for manuscripts on which they were an author.

https://doi.org/10.1016/j.actbio.2022.08.051

still represent a major challenge due to their size, often complex shapes and limited tissue availability [1]. An alternative solution to overcome the limited supply of autografts is the use of allografts. However, allografts carry the risk of rejection and transmission of diseases, which may result in failure to integrate within host tissue [2,3]. Bone tissue engineering strives to serve as a platform to overcome the shortcomings and complications associated with autologous and allogeneic bone grafting. This multidisciplinary field combines the principles of materials science, biomechanics, cell biology, and medical sciences and requires collaborative efforts of scientists, engineers, and surgeons to achieve the ultimate goal of developing a biologically compatible and functional engineered bone constructs [4]. In this context, a functional bone construct should eventually integrate with adjacent host bone and vascular supply, and ultimately perform the functions of native bone as a load-bearing tissue that is primarily involved in locomotion [5,6]. The ability to create a functional bone tissue engineered construct with the capacity to maintain homeostasis would revolutionize the way bone defects will be treated in the clinics. By implementing computer-assisted imaging and preoperative planning, customized grafts with desired shape and dimensions could be fabricated allowing for personalized bone reconstruction [7].

Over the past three decades, significant strides have been made in the field, from the incorporation of cells with or without growth factors within scaffolds to the development of “smart” biomaterials with specific osteoinductive properties [8–10]. While bone tissue engineering has celebrated some successes in the reconstruction of bone defects in various animal models [11–18], upscaling to larger clinically relevant sizes (1-10 cm^3) still presents a major hurdle. The lack of effective strategies to fully vascularize the constructs, especially down to their core, has limited the survival and success of cell-laden, three-dimensional (3D) tissue engineered bone constructs after implantation. In fact, the main causes of construct failure are necrosis and lack of integration with the host tissue [19]. It is also known that the processes of bone formation and vascularization are closely intertwined, and ossification cannot take place in the absence of vascularization [20]. Cells need to be within 100 to 200 µm of blood vessels in order to survive [21] and unfavourable hypoxic conditions can impact the secretome of the affected cells impairing tissue homeostasis and consequently the regenerative process [22]. Moreover, vascular supply also serves as a conduit to recruit various cell types involved in the inflammatory response required to complete bone regeneration and in construct remodelling and integration.

Without a readily perfusable vascular network, the current size of a tissue engineered bone construct is theoretically limited to about 400 µm in at least one dimension, impeding clinical translation of larger, more complex bone tissue engineered constructs [23]. *In vivo*, neovascularization occurs via vasculogenesis and/or angiogenesis. This arises from close association between differentiation of precursor cells into endothelial cells (ECs) to form vascular structures or from the sprouting of pre-existing blood vessels, respectively [24]. Classical approaches to tissue engineering sought to prevascularize a construct before implantation to overcome the diffusion limitation. To induce vasculogenesis *in vitro*, a multitude of strategies have been explored using a variety of endothelial lineage cells in combination with supporting cells (i.e. acting as pericytes). A thorough overview of standard cell types used for *in vitro* prevascularization has recently been published [25]. While *in vitro* prevascularization with co-culture models in combination with biomaterials have exhibited some degree of success (e.g. accelerated inosculation with host capillaries) for constructs of millimetre-scale dimensions [26], clinical translation of these studies is still hindered by significant design limitations and challenges associated with upscaling to larger, centimetre-sized tissue-engineered bone constructs [27]. Firstly, microvascular structures need perfusion to maintain viability of cells and drive maturation *in vitro* within a large fabricated 3D tissue engineered construct. Thus far, a majority of studies have focused on generating microvascular networks without any attention to the spatial organization of formed microvessels, thereby failing to provide a natural inlet and outlet for perfusion during preculture in the lab or for *in vivo* anastomosis [28–31]. Secondly, inosculation with host capillary bed takes at least 48 hours resulting in reliance on diffusion for nutrient transport during this period, which is inadequate when upscaling to larger constructs [32,33].

In recent years, the field of biofabrication has shown great promise in developing more complex, native-like structures for a wide array of tissue engineering applications, owing to the precise spatial patterning of biomaterials and cells through the use of additive manufacturing technologies, such as 3D printing [34]. Biofabrication techniques offer a wide range of achievable resolutions and printable biomaterials, which can directly or indirectly incorporate living cellular components into the printed constructs (Table 1). These are particularly interesting in the fabrication of tissue mimics that possess a more hierarchical vascular architecture for accommodating tissue metabolic needs [35]. Importantly, tissue engineered grafts must undergo maturation before attaining full functionality, and the intricate spatial patterning facilitated by these biofabrication approaches can help accelerate this process [36]. The high degree of freedom of design and geometric accuracy both at a macro- and microscale level has allowed for the biofabrication of vascular-like structures with increasing levels of success. The aim of this review is to explore some of the breakthrough biofabrication approaches on vascularization for the generation of a hierarchical vascular network are explored. To address this, different strategies employed in the fabrication of macro (1000 -100 µm) and micro (< 100 µm) scale vessel-like structures with different resolution ranges are highlighted. This review will provide key perspectives on the potential and limitations of existing research in biofabrication of vascularized tissues. Lastly, vascularization approaches specifically for bone tissue engineering are explored and challenges and current solutions, as well as future perspectives are discussed.

2. Defining the vascular network

In addition to oxygen and nutrient delivery, the vascular system is instrumental in regulating bone formation and bone marrow hematopoiesis [37]. ECs are composed of a heterogenous population of subtypes with specialized functional properties in specific local microenvironments [38]. For example, osteogenesis is supported by type H capillary ECs and the sinusoidal vessel network of the bone marrow is regulated by type L ECs. Type H capillary ECs support bone formation and bone growth via angiocrine signaling of osteogenic factors and mediate angiogenesis in bone both during developmental and regenerative stages [39]. In concert with the vascular system, the skeletal system is a hierarchical system composed of MSCs, osteoprogenitors and osteoblasts which regulates lifelong bone formation [38,40]. During bone development and regeneration, the migration of osteoprogenitor cells and osteoclasts to the defect site ensues vascular invasion. Together, these two systems work in synchrony to regulate bone formation and homeostasis. The release of VEGF from bone forming cells not only influences ECs, but also affects the function of other cell populations such as chondrocytes, osteoblasts and osteoclasts [41]. In parallel, ECs secrete pro-osteogenic factors, e.g. BMP-2, which stimulate osteoblasts. Recapitulating the full range of resolution, structure and function displayed by native vasculature has been a major challenge in the fields of tissue engineering and biofabrication to date. While major breakthroughs have been made for large diameter (> 8mm) and medium-diameter arteries (6 - 8 mm) through the in-

Table 1
Advantages and limitations of different bioprinting techniques for the purpose of fabricating vascular structures outlined throughout this review, classified according to printing category based on their working principles.

Printing category	Technique name	Advantages	Disadvantages	Refs.
Extrusion-based bioprinting	Sacrificial printing	- Simple process that can be performed with conventional 3D bioprinting equipment - Allows for the fabrication of interconnected 3D hollow networks - Printing of multiple materials (sacrificial and cell-laden biomaterials) - Void-free sacrificial printing allows for more homogenous channel seeding	- Channel resolution largely dependent on nozzle diameter (>100um) - Complex, out of plane structures are very challenging to achieve. Only possible with support materials that increase printing time significantly	[49,50]
	Co-axial printing	- A single nozzle can be used to create multilayered hollow channels - Different materials and cells can be processed through distinct printing parameters for each nozzle layer - Hierarchical tubular structures are achievable in a single process	- Channel resolution largely dependent on nozzle diameter (>100um) - Complex, out of plane structures are very challenging to achieve without the use of support materials - Specialized nozzles necessary, as well as multiple pressure sources for each layer that can be independently controlled	[51,58]
	Suspension bath printing	- Allows for the fabrication of complex, overhanging and out-of plane 3D structures given the structural support provided by the bath around the extruded material - Soft and low viscosity materials can be printed with high accuracy given the surrounding support bath	- Feature/channel resolution largely dependent on nozzle diameter (>100µm) - Optimization of support bath and extrusion material properties is essential to ensure homogenous filament printing - Removal of support bath can damage small, fragile structures and result in low shape fidelity	[54–56,58]
	SWIFT Sacrificial suspension bath printing	- Allows for the fabrication of complex, overhanging and out-of plane hollow 3D structures given the structural support provided by the bath around the extruded material - The support bath can be composed of cell (and spheroids) slurries, thus allowing all the benefits of embedded printing in a construct with very high cell densities		[57]
Inkjet printing	Drop-on-demand (DoD) printing	- Precise deposition of cell-laden biomaterials capable of self-assembly into hollow vessel-like structures - Can achieve single-cell resolutions, for more controllable vessel sizes	- Challenging to fabricate complex 3D structures through this technique alone, convergence with other methods necessary for hierarchical architectures is needed	[142–144]
Acoustic wave patterning		- Low shear stress approach that allows for patterning of cell-laden biomaterials in a wide array of architectures - Through self-assembly, microvascular structures can be achieved that exhibit directionality based on wave frequency and pattern.	- Challenging to create hierarchical 3D constructs - Effect of soundwaves on cellular processes needs further investigation	[106,107]
Light-based bioprinting	Stereolithography and digital light processing	- Allows for printing of hollow, highly convoluted structures without the need for support materials - Printing resolutions allow for a wide array of vessel types to be printed (>5µm) - Nozzle-free printing approach does not expose cells to shear-stresses typical of extrusion-based techniques	- Limited to photocrosslinkable biomaterials - Addition of photoabsorbing compounds necessary to achieve higher resolutions - Convergence of multiple materials or printing approaches is challenging, and requires substantial technical modifications to conventional systems	[67-69,71].

(*continued on next page*)

Table 1 (*continued*)

Printing category	Technique name	Advantages	Disadvantages	Refs.
	Two/multi-photon laser ablation	- Can achieve resolutions in the nanometer scale, especially attractive for printing capillary-like structures - Iterations of the technique allow for *in situ* printing to remodel vessel networks at different time points during culture - Nozzle-free printing approach does not expose cells to shear-stresses typical of extrusion-based techniques	- Time consuming process given the extremely high resolutions that can be achieved, which can result in detrimental effects on cell viability and function - Patterning multiple materials in a single process is challenging to requires technical modification to conventional systems Given the speed of the technique, the ability to build large and complex 3D structures is limited	[96-98,103,104,108]
	Volumetric bioprinting	- Fastest bioprinting approach to date (10s of seconds) - Allows the contactless fabrication of centimeter-scaled constructs, making it possible to maintain cell/organoid morphology and viability during and after printing - Its single-step approach allows the fabrication of convoluted, hollow channels and free-floating components	- Current resolution of negative features is >100μm - Introduction of high cell densities requires material or software adjustment to improve resolution - Patterning multiple materials in a single process is challenging to requires technical modification to conventional systems	[146–149]

troduction of synthetic grafts, the same cannot be said for small-diameter vascular grafts (<6 mm), which have consistently shown poor success rates due to surface thrombogenicity and intimal hyperplasia [37,38]. The introduction of biofabrication has revolutionized the way in which small diameter vascular grafts can be manufactured [39]. However, the generation of small diameter vascular grafts (1 – 6 mm) for the application of cardiovascular surgery is beyond the scope of this review and a comprehensive up-to-date review is provided elsewhere [40].

2.1. Establishing a vascular foundation: The biofabrication of perfusable macrochannels

The incorporation of macrochannels with diameters ranging from 100 – 1000 μm within a tissue engineered construct can allow for perfusion, support mass transport and partly overcome the limits of nutrient and oxygen exchange during the *in vitro* culture steps. Earlier approaches to introduce such channels included various templating techniques, which required manual labour with tubing or blunt needles. This process was not only time consuming but was also limited to the generation of linear channels that do not reflect the out-of-plane complexity of a vascular network [41–44]. Taking the principle of templating to a more architecturally complex level, multiple research groups have turned to sacrificial printing [45–48]. Here, a desired 3D pattern is first printed as a vascular template using a fugitive ink. Next, a second (bio)ink is manually casted or printed around this sacrificial template, and the fugitive ink is removed from the construct, resulting in open tubular structures that span throughout the (bio)ink. The hollow tubular structures are then typically manually seeded with ECs to create endothelialized channels and, if desired, are then perfused with media to facilitate diffusional mass transport and drive tissue maturation throughout the entire construct. In a hallmark study, Kolesky and colleagues demonstrated for the first time the feasibility of creating thick prevascularized tissues (≥1 cm) within customized perfusion chips through sacrificial printing (Fig. 1A) [49]. The group demonstrated the ability to print macrochannels of approximately 200-300 μm in diameter that could be seeded with ECs and maintained in long-term culture for up to 45 days (Fig. 1B). Based on this same working principle, the study also fabricated more complex endothelialized microchannel networks to sustain tissue function and maturation in thick structures and provided new insights in the capabilities of printing more complex, 3D prevascularized structures through the use of sacrificial materials.

Initially, sacrificial printing approaches were limited to post-seeding of ECs to create endothelialized lumina, which is often inefficient and can result in non-uniform distribution of cells. Ouyang et al. sought to overcome this by using a void-free 3D printing (VF-3DP) approach by pre-loading ECs into a sacrificial gelatin bioink permitting *in situ* endothelialisation (Fig. 1C-F) [50]. To achieve this, gelatin-based templating bioink pre-loaded with ECs and a photo-crosslinkable matrix bioink (Gelatin Methacryloyl; GelMA) were printed in a side-by-side manner to form a void-free 3D structure. Following photocrosslinking of GelMA, the thermoreversibly crosslinked templating bioink was liquefied at 37°C, resulting in *in situ* seeding of cells. Their single-step approach was found to have close to a 3-fold improvement in seeding efficiency in comparison to post-printing seeding [50]. Applying this approach could also be an efficient way to reduce the amount of cells needed to seed channels, which is key when upscaling to clinically-relevant sized constructs that require high cell yields. Drawing from a similar one-step approach, Shao et al. demonstrated the printing of complex anatomical 3D structures using a 2-in-1 system combining co-axial and sacrificial printing (Fig. 1G-H). The co-axial system consisted of an inner EC-loaded gelatin sacrificial ink, and an outer channel which consisted of cell-laden GelMA that was covalently cross-linked after extrusion [51]. As already demonstrated in previous work, dissolving the gelatin led to the release of ECs that adhere to the luminal interior of the channels creating vascular-like structures [51]. Depending on the cell type encapsulated within the crosslinked GelMA bioink, this approach can be tailored for the construction of various vascularized tissues. These one-step seeding systems certainly overcome one of the major drawbacks associated with upscaling in sacrificial printing approaches, namely the inefficient cell seeding process required to create endothelialized channels from these printed templates.

The aforementioned extrusion-printing approaches, however, pose some design limitations that prevent complete recapitulation of native vasculature in a 3D environment, specifically in capturing complex, out-of-plane vascular networks. Gravity tends to distort the soft biomaterials needed for EC survival and optimal function before they can be cross-linked into the desired or extruded

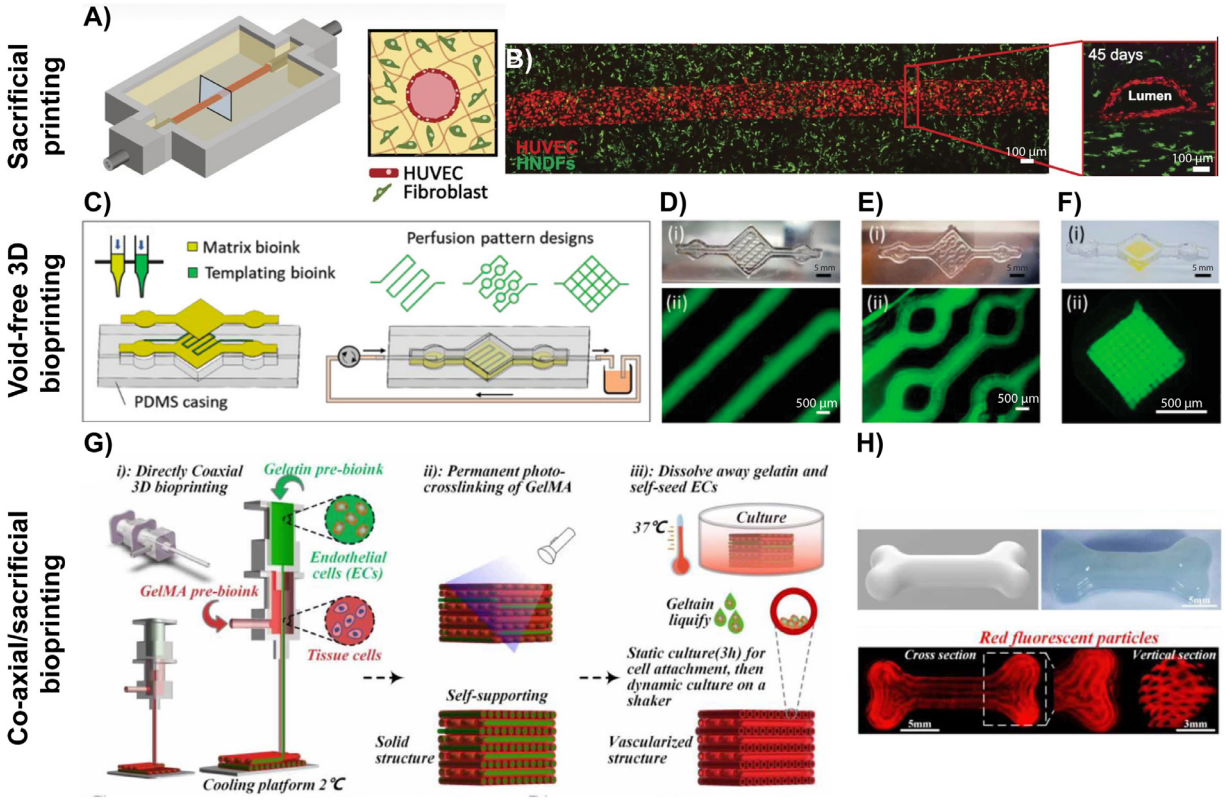

Fig. 1. Sacrificial bioprinting approaches for the fabrication of macrochannels in engineered bone tissues. A) Schematic of a single sacrificially printed channel lined with human umbilical vein endothelial cells (HUVECs) within a casted fibroblast (HNDF)-laden matrix placed inside a perfusable chip system. B) Confocal images of the endothelialized channel (red = HUVECs) and the surrounding HNDF-laden matrix (green) after 45 days of culture, and a cross-sectional image of the channel showing the hollow-nature of the channel; images reproduced with permission from [49]. C) Schematic of void-free bioprinting approach in which channel seeding efficiency is enhanced by placing the endothelializing cells in a sacrificial, templating bioink that is printed within a matrix bioink in different patterns within a perfusable chip system. D) Straight an S-shaped channel path, E) S-shaped channel with circular junctions and a F) 3D lattice imaged i) optically in the perfusable system, and ii) fluorescent images of a perfusing dye through the open channels created with the templating sacrificial ink; images reproduced with permission from [50]. G) Schematic of a hybrid approach combining co-axial and sacrificial, void-free bioprinting, in which the outer shell of the printed filament contains the target tissue cells in a crosslinkable bioink and the inner shell contains a sacrificial templating bioink that permits void-free endothelialization of the fabricated channels upon washing of this inner channel ink. H) 3D model of a simple bone model and the resulting prevascularized co-axially printed structure; images reproduced with permission from [51].

geometry [52,53]. Adapted by a method known as embedded 3D printing (e-3DP) described by the Muth et al. [54], Hinton et al. introduced Freeform Reversible Embedding of Suspended Hydrogels (FRESH) which utilizes a high-density bath composed of sacrificial, thermoreversible gelatin particles, that keeps the printed bioink in place until stabilization (Fig. 2A-B) [55]. FRESH printing allows the high-fidelity printing of soft materials by employing Bingham-plastic and/or self-healing support bath materials, capable of reversibly fluidizing due to the shear stresses elicited by the extrusion process while supporting the extruded bioink post-printing [55,56]. This allows for the freeform fabrication of out-of-plane structures with resolutions of up to 200 µm, that can better mimic tissue complexity [55]. In the following years, a new variation on this approach was introduced to fabricate 3D vascularized tissues with the cellular density and microstructural complexity of native tissue, via the a method termed sacrificial writing into functional tissue (SWIFT) (Fig. 2D-F) [57]. This revolutionary, modular approach consists of a compact matrix of so-called organ building blocks (OBBs, made from jammed spheroids or embryoid bodies), which make up the supporting bath in combination with a matrigel and collagen I solution and thus enable freeform printing. A vascular template is then printed into this living matrix using gelatin as a sacrificial ink and consequently removed at physiological temperature to generate a perfusable network of tubular channels. The presence of vascular channels not only preserved the viability of the OBBs, but also stimulated tissue maturation of the 4 mm thick living tissue that was made up of approximately 500 million cells at a cellular density of 200 million cells/ml. In contrast, non-perfusable controls, devoid of the gelatin-derived vascular templates, exhibited a necrotic core within 12 hours due to diffusion limitations; confirming the functionality of the printed channels. The group also generated a bifurcated vascular network in a simpler SWIFT construct that was seeded with EC, however they were not able to achieve a confluent endothelium at this time [57]. While the model is still in its early stages and requires significant optimization in printing resolution, as well as elaborate characterization of the endothelialization of the open channels, this approach has demonstrated enhanced architectural complexity of vascular networks for volumetric tissue mimics compared to conventional extrusion printing methods.

Many techniques aiming at vasculature biofabrication rely on the printing of (endothelialized) channels as vessel templates, but this approach alone, focusing on the inner, endothelial lining of the vessel only, does not take into account the anatomical structure of the non-capillary segments of the vasculature that are composed of *the tunica intima, tunica media* and *tunica externa*, which contribute to the overall functioning of a vessel. To address this, co-axial printing systems have proven to be highly versatile, as through simple modification of the channels, the coaxial extruder permits the fabrication of complex cylindrical structures, that are layered with different bioinks according to the design of the different nozzle compartments. Dikyol et al. demonstrated the feasibility

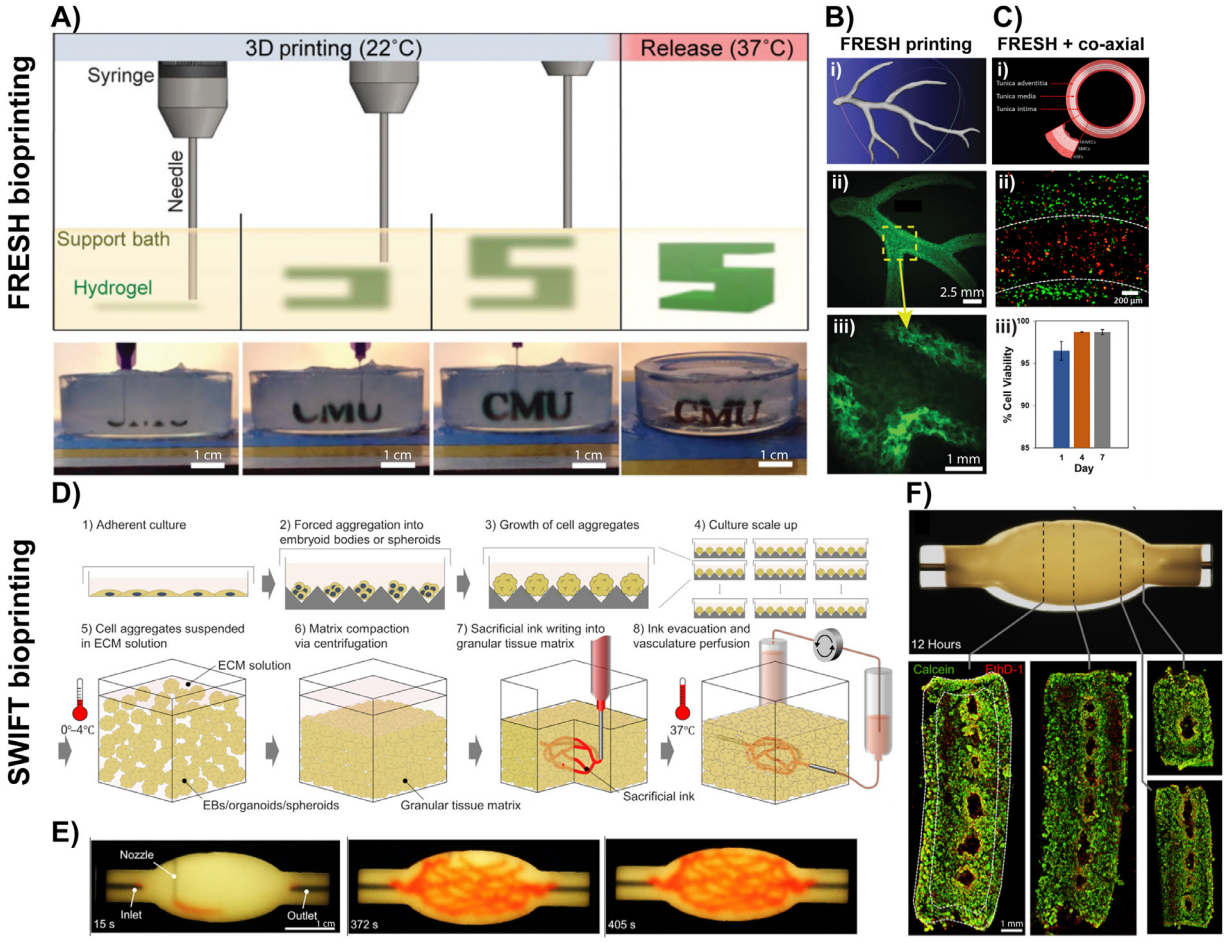

Fig. 2. In-bath printing approaches for the fabrication of macrochannels. A) Schematic and optical images of the FRESH bioprinting approach, in which a soft bioink can be accurately printed inside a support bath/granular tissue matrix that enhances shape fidelity and allows for nonplanar extrusion printing. Bi) 3D MRI model of a region of the human right coronary arterial tree ii) printed via FRESH approach with fluorescent alginate and iii) imaged in 3D to show the hollow lumen achieved through this printing technique; images reproduced with permission from [55]. Ci) A combination of FRESH and coaxial printing allows the printing of hollow, multi-layered macrovessel structures, showing ii) distinct multicellular layers from each layer of the printing nozzle, and resulting in iii) sustained high cell viability post-printing; images reproduced with permission from [58]. D) Schematic of SWIFT printing approach, in which a sacrificial bioink is printed within a cell/aggregate-laden support bioink. The sacrificial ink can be removed post-printing resulting in open, perfusable channels. E) Sequential optical images of the embedded printing process of the sacrificial ink within the aggregate-laden tissue matrix to create a complex, nonplanar vascular network. F) Multichannel construct of a hierarchical vascular network printed via SWIFT approach, showing that the fabricated channels span through the entire length of the construct after 12 hours of perfusion;; images reproduced with permission from [57].

of creating layered structure by using a multi-material bioprinting platform to fabricate biomimetic vascular constructs via co-axial printing [58]. Through the incorporation of 3 different bioink formulations consisting of ECs, smooth muscle cells (SMCs) and human skin fibroblasts (HSFs), the research group was able to mimic the *tunica intima, media* and *externa* of an abdominal aorta, respectively (Fig. 2C). The bioinks were simultaneously extruded through a multi-channel nozzle into a support bath, which facilitated the controlled movement of the nozzle and provided support to the extruded bioink prior to crosslinking. Trying to mimic the native aortic wall thickness, researchers achieved layers of between 250 – 835 µm, showing approximately 10% thicker walls than native structure, but keeping to the thickness ratio exhibited by the three different vessel layers. This multi-material printing approach could serve as a platform for the biofabrication of more structurally complex, tissue engineered vascular networks.

While extrusion-based techniques have been the most widely used biofabrication approaches to date and have shown promising developments in the field of vascular tissue engineering, their working principle poses some significant drawbacks. Firstly, the extrusion process imposes shear stresses on cells when being deposited out of the nozzle, a potentially harmful factor that can impair biological functions and cell viability [59]. This nozzle-based approach also limits achievable printing resolutions (as nozzle size and the ensuing Barus effect observed in most of the non-Newtonian fluids that possess the shear-thinning quality essential for extrusion to occur) [60]. Even under optimized printing parameters, this often results in extruded filaments with similar sizes as the inner diameter of the employed nozzle. Considering that the smaller the nozzle, the greater the shear stresses imposed on the printed cells, this limits the printing resolution of extrusion techniques to hundredths of micrometers. Another class of biofabrication approaches that circumvents these limitations are light-based approaches, which rely on photocrosslinking or photodegradation of spatially controlled regions of photosensitive resins to create complex 3D objects [61]. This category of printing approaches offers a wide range of printing resolutions depending on the specific process and illumination method, from the nano- to centimetre scale. Additionally, these nozzle-free approaches do not expose materials and cells to shear stresses, making them more suitable for printing complex multi-scale systems with minimal impact on cell viability. Given the mechanisms of the photochemical reactions typically occurring in light-based printing, potential risks for embedded cells due free-radicals have been extensively

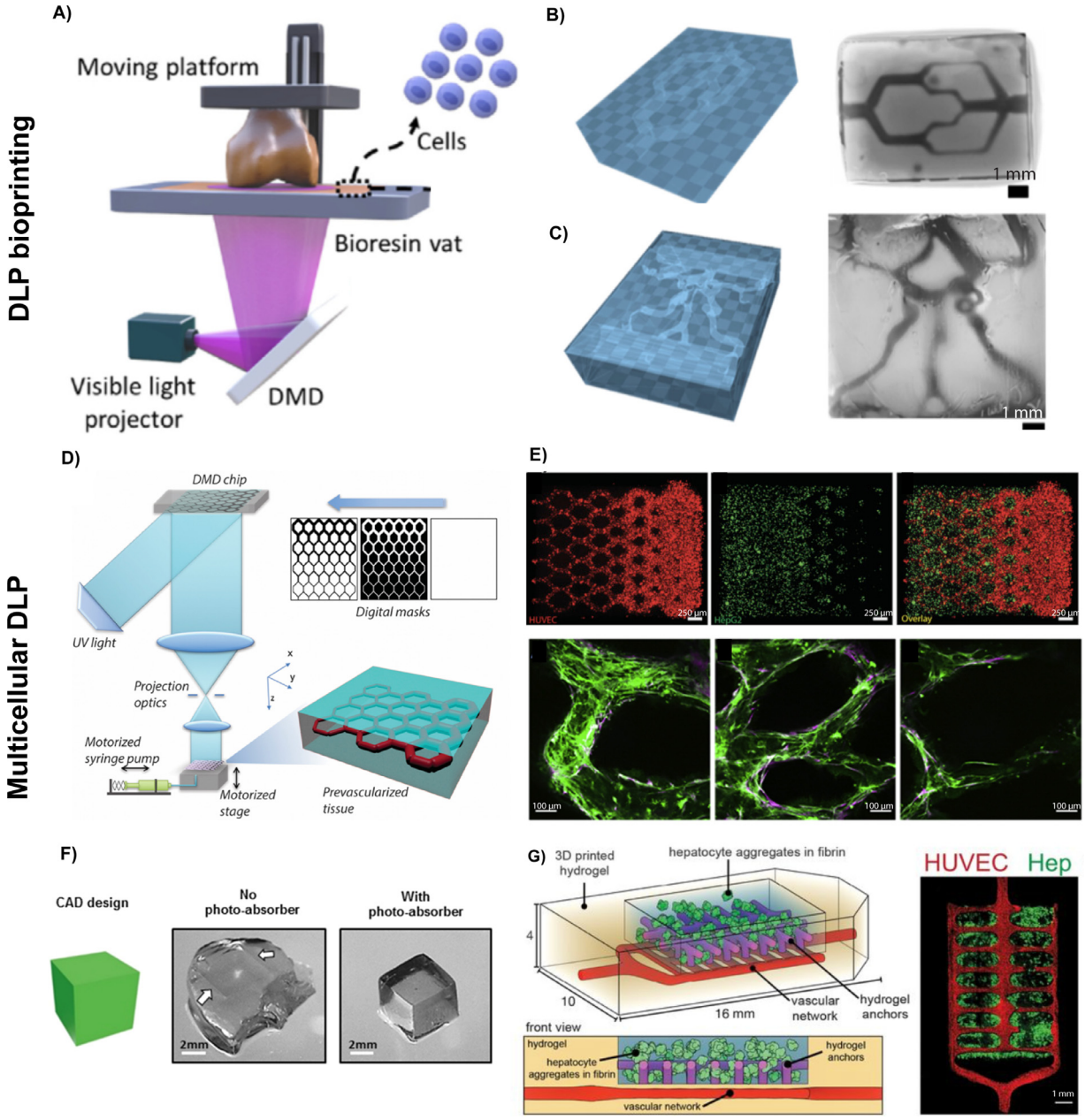

Fig. 3. Light-based biofabrication strategies for complex macrochannel formation. A) Schematic representation of the DLP process in which a photosensitive bioresin is cured in a layer by layer fashion through the sequential projection of photomasks of the desired 3D object. B) Complex perfusable microfluidic chip structures with a range of different channel diameters and C) convoluted, non-planar channels mimicking a region of blood vessels in the human Willis circuit can be successfully printed with this approach; images reproduced with permission from [67]. D) The ability to project different photomasks onto different photosensitive resins in a sequential manner allow for the creation of multimaterial and multicellular structures. E) Bioprinted cellular construct with HUVECs (red) and HepG2s (green) encapsulated in different printed regions of the 3D construct, showing vessel-like channels of different diameters throughout the print. Below, a vascular co-culture of HUVECs (green = CD31-positive) and 10T1/2 cells (purple = αSMA-positive) show endothelial network formation after 1 week of culture, exhibiting different vessel sizes as determined by the initial design of the printed structure; images reproduced with permission from [70]. F) DLP printing resolution can be enhanced through the use of photoabsorbers, resulting in highly accurate prints compared to the computer-generated 3D model; images reproduced with permission from [71]. G) DLP-printed, perfusable vascular-like network seeded with HUVECs and surrounded by hepatocyte aggregates embedded in fibrin gel was implanted and demonstrated albumin production *in vivo*; images reproduced with permission from [68].

studied [62,63]. Experimental data from several groups indicate the safety of the process, with careful selection of photo-initiator concentration, and light doses and wavelengths [64,65]. For the generation of macro-scale vessel structures, the use of digital light projection (DLP) strategies has enabled the fabrication of out-of-plane, highly complex vascular structures (Fig. 3A). A wide array of light-responsive, biocompatible polymers has been used to create self-contained, vascularized chip models (Fig. 3B) [66,67], anatomically accurate vascular networks (Fig. 3C) [67,68] and vascularized, multicellular tissue models (Fig. 3D-E) [69,70]. To improve the resolution of this versatile printing approach, synthetic and natural dyes that act as photoabsorbers at the peak absorption wavelength of the photoinitiator system have been used, allowing the resolution of features in the range of 5 – 100 µm (Fig. 3F) [67,68,70,71]. Interestingly, many of these water-soluble photoabsorbers, suitable to be used in hydrogel-based bioresins, are well known biocompatible food dyes [71]. In an impactful study in the area of vascular bioprinting, Grigoryan et al. utilized a photoabsorbing

compounds to manufacture complex functional macrochannel networks, and developed a proof-of-concept, vascularized system carrying mouse hepatocytic spheroids with EC-seeded channels. To validate their translational potential, the prevascularized hepatic hydrogel carriers were implanted into a rodent model of chronic liver injury. Impressively, the carriers not only survived transplantation but also exhibited albumin production indicating survival of functional hepatocytes (Fig. 3G) [68]. The interconnected networks produced with this approach could be potentially applied to other tissues, and for instance implemented in a large tissue engineered bone construct. The continuous development of a wide array of extrusion- and light-based bioprinting approaches will facilitate the fabrication of macrochannels with increasing architectural complexities. However, while these macrochannels form the foundation of engineered vascular networks, an open challenge still remains when reconstructing channels on a micro-scale to represent the capillary bed.

2.2. Engineering capillary beds: strategies for the fabrication of a defined network of capillaries

In the early years of tissue engineering, the main approach to vascularize a construct relied solely on the ingrowth of host capillaries after implantation *in vivo* [72]. This led scientists to explore techniques which would promote and accelerate rapid host capillary ingrowth upon implantation such as functionalization of scaffolds with angiogenic growth factors [73–77]. Alternatively, scaffold design *i.e.*, surface topography, porosity, pore size and pore interconnectivity are other well-known factors to affect vascular cell behavior and degree of vascular invasion [78–84]. While these approaches can eventually lead to the formation of a mature vasculature, the slow rate of host capillary invasion limits the practicality of this approach for larger constructs containing living cells. After all, it is estimated, based on *in vitro* studies on angiogenesis, that capillaries have an average sprouting rate of 5 μm/hour - meaning vascular ingrowth would be limited to less than 1 mm of scaffold penetration per week, resulting in cell necrosis in the core [85].

As ECs are capable of self-aggregating and forming capillary-like networks *in vitro,* researchers explored the possibility of generating a vascular network prior to implantation as means to decrease the time required to vascularize a construct *in vivo* [86–89]. Through advancements in understanding of the natural process of neovascularization in embryologic development, several researchers cultured ECs to generate microvascular-like structures *in vitro*. Studies later confirmed that cultivation of ECs in combination with perivascular cells was pivotal in generating long lasting microvascular networks [27,90]. While *in vitro* prevascularization with co-culture models in combination with biomaterials have exhibited some success (e.g. inosculation with host capillaries) for constructs of small dimensions, the translation of these studies are far in the horizon due to the significant design limitations and challenges associated with upscaling to larger, centimetre-sized constructs. The cultivation of ECs relies on random microvascular formation to generate rudimentary microcapillaries, which cannot support perfusion and mass transport of nutrients. As a result, the size of a prevascularized construct is still restricted by diffusion limitation [32,33].

Conversely, in recent years, microfabrication, originally introduced for semiconductor manufacturing, has proven to be a powerful tool in microvessel engineering [91]. Able to resolve features as small as 0.1 μm (which is approximately two orders of magnitude smaller than the dimensions of native capillaries), microfabrication technology permits the generation of a microcirculatory network blueprint to be built within a tissue engineered scaffold [92]. Another relevant application of microfabrication approaches is the creation of microfluidic devices, which allow for the highly controlled perfusion of microchannels, and can more closely mimic cellular microenvironments. Since their introduction, microfluidic devices have been produced via soft lithography [93,94], additive manufacturing [95], photolithography [96–98] and micro-molding [92] processes, which are often limited to planar microfluidic networks. While initial microfluidic devices were limited to non-biodegradable poly(dimethylsiloxane) (PDMS) [99] and silicone [92], which do not permit native tissue remodelling throughout the construct to take place, recent work has shifted towards more biocompatible and biodegradable elastomers for the generation of microcapillary-like networks [100–102]. Using laser-based photodegradation, in which a pulsating laser beam elicits hydrogel degradation in a spatially controlled manner, leading to the formation of open channels, Brandenberg et al. generated negative features in the micrometer-range within a biocompatible collagen hydrogel [103]. This light-based system allows for *in situ* patterning of complex channels whilst the 'no contact' approach preserves the sterility of the encapsulated cells during the manufacturing process, exhibiting potential for *in situ* bioprinting strategies to directly integrate capillary networks into defect sites (Fig. 4A-D) [103]. This laser-based hydrogel photodegradation principle has been further combined with image-guided laser control generate highly tortuous and out-of-plane 3D networks within microfluidic devices [104,105]. Heintz et al fabricated pre-defined channels for endothelialisation within poly(ethylene glycol) diacrylate (PEGDA) hydrogels [104]. This precise approach generated independent, intertwining channels that come within 15 μm of each other without directly connecting, recapitulating *in vivo* vascular architecture. Furthermore, the non-planar, capillary-like networks (average diameter of 8.1 ± 2.2 μm) supported endothelialisation and displayed inter-network transport in close proximity via the hydrogel. This approach most certainly opens new avenues for creating complex vascularized tissues in the field for a multitude of applications.

More recently, acoustic wave patterning has garnered significant interest to regulate the orientation and local distribution of ECs for the generation of a pre-vascularized construct. Acoustic vibrations are used to generate a pressure gradient in a fluid (e.g. an uncrosslinked hydrogel) to allow for precise patterning of suspended cells in a fast and contactless manner (Fig. 4E) [106]. This approach overcomes several drawbacks associated with microfabrication such as loss in cell viability due to shear stress and long manufacturing times. Using an acoustophoretic fabrication system, Kang et al recapitulated the pattern of cells at distances reflecting inter-capillary distance in human skeletal tissue [106]. The alignment of cells increased local cell density which in turn enhanced cell-cell contact, promoting the patterned fusion of ECs into microvessels (Fig. 4F). The therapeutic potential of the vascular pattern was evaluated in an ischemic hind limb injury model in a mouse. After 28 days, the 3D-patterned alignment of cells within the hydrogel displayed integration with host vessels, producing functional microvessels thereby restoring blood flow and significantly improving ischemic limb salvage with reduced necrosis in the feet and limbs [106]. Similarly, Petta et al. used an acoustic patterning method with Faraday waves to spatially pattern ECs and mesenchymal stem cells (MSCs) to generate a perfusable microvascular network *in vitro* within a fibrin hydrogel [107]. By optimizing parameters such as amplitude, frequency of sound waves and chamber geometry, they were able to spatially control the patterning of cell densities within a hydrogel (Fig. 4G-H). Their approach not only generated *in vivo*-like microvascular structures in the laboratory but also accomplished this with far less cells in comparison to more conventional approaches such as microfluidics. However, while this cutting edge technique shows great promise, this field of research is still in its infancy. More long term studies are required to fully elucidate the effect of acoustic manipulation on

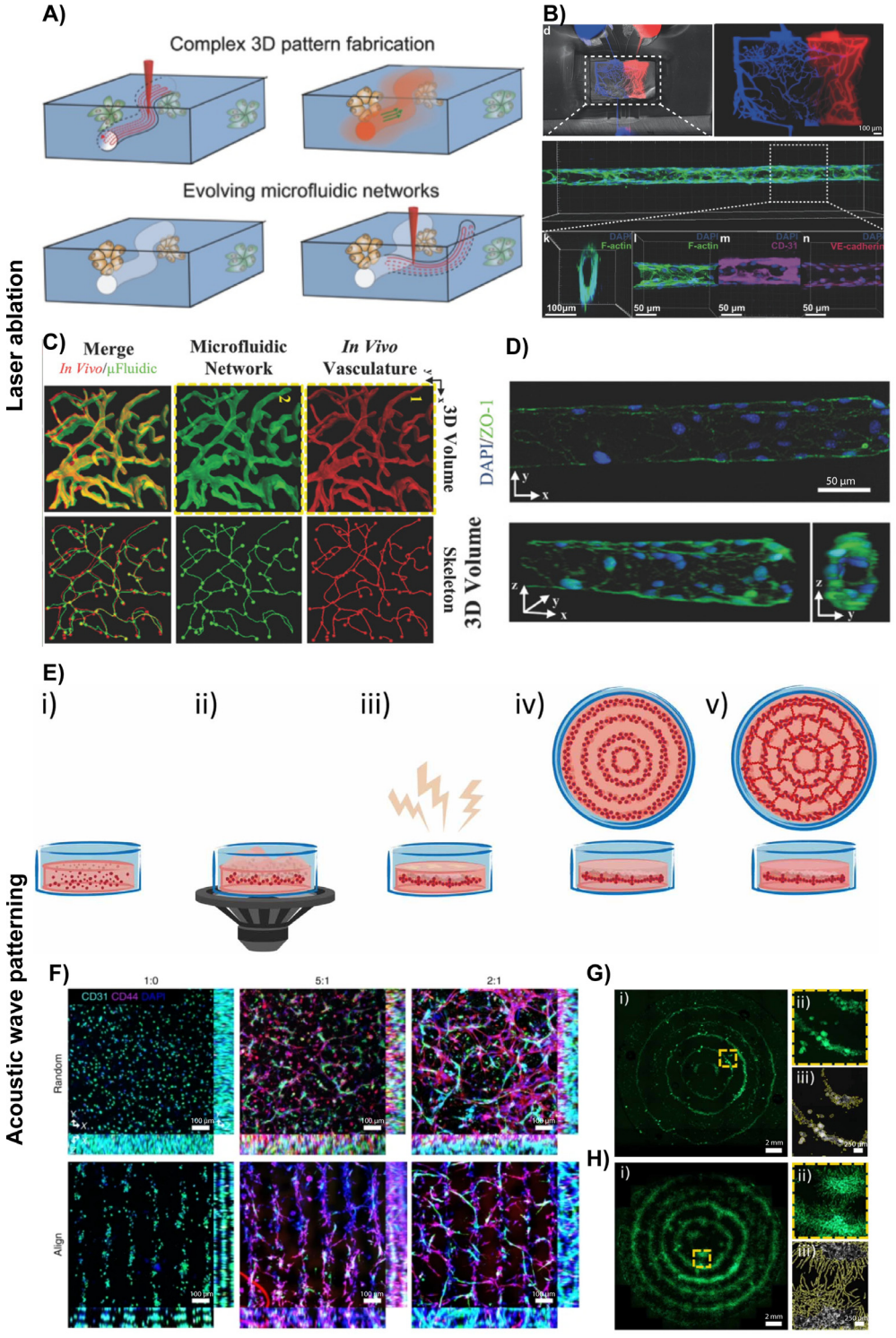

Fig. 4. Micro-channel fabrication strategies for capillary bed formation. A) Schematic of *in situ* laser-based hydrogel photodegradation process, showing the ability to create open channels by scanning specific locations of a hydrogel construct. Additional channels can be added during culture through *in situ* processing. B) This process can yield highly complex perfusable vascular networks, mimicking arteriovenous circulation. Confocal 3D reconstructions of endothelialized channels created through this approach show expression of vessel markers V-cadherin and CD31; images reproduced with permission from [103]. C) 3D vascular-derived microfluidic networks created through laser-based photodegradation show high printing accuracy compared to native vasculature. D) Microchannels were homogenously seeded with mouse brain endothelial cells; images reproduced with permission from [104]. E) Schematic overview of sound-induced morphogenesis process, in which acoustic waves are used to pattern cells within a biomaterial in spatially controlled architectures in a contactless manner; images reproduced with permission from [107]. F) The effect of acoustic wave patterning-based cell alignment on vascular growth and alignment was demonstrated using a co-culture of HUVECs and human adipose-derived stem cells, showing an increase in vessel alignment and interconnectivity between channels in the acoustically-patterned group; images reproduced with permission from [106] G) HUVEC/mesenchymal stem cells (MSC) aggregates were patterned in a circumferentially aligned fashion and exhibited capillary bed growth after H) 5 days in culture, exhibiting sprouting and creating interconnections between the different circumferential struts of the construct; images reproduced with permission from [107].

cell function and signaling. While the introduction of biofabrication has most certainly overcome the limitations associated with traditional co-culture approaches such a lack of perfusion and uncontrolled microvascular organization, these microvascular structures do not represent the multi-scale nature of native vasculature. Furthermore, the size and dimension of these microvascular structures do not permit direct surgical anastomosis to host vasculature to allow for immediate reperfusion of the tissue engineered construct, therefore exclusively relying on spontaneous anastomosis with host capillary bed.

2.3. Branching out the vascular network: the need for integration between macro- and microvascular network to create an interconnected hierarchical vasculature

The human vascular system consists of a complex network that runs throughout the body in a tree-like hierarchical branching fashion consisting of larger vessels (macro-vessels) with multiple sprouting vessels (microvessels) that interconnect to form a closed network. A majority of studies thus far has focused on creating a vascular network either on a macro- [49,55,57,58] or micro-scale [103,104,106] alone. However, in order to maintain the viability of a thick engineered construct, these two scales of vasculature need to be integrated to form an interconnected system. Arakawa et al. elegantly described the generation of interconnected channels ranging from 300 µm down to 25 µm to recapitulate the complex hierarchical vascular geometry via multiphoton lithography. This laser-based approach uses a multiphoton laser to scan through a resin volume and elicits a chemical change at the focal point of the photons employed, thus creating non-planar, high-resolution structures - in this case, by selectively photodegrading resins to create open channels (Fig. 5A-C) [108]. To study the complex 3D flow profiles inside the network and to demonstrate scalability, they fabricated centimetre-sized fluidic networks of up to 1.2 cm depths via photodegradation of a PEG hydrogel functionalized with o-nitrobenzyl moieties and manipulated channel curvature to improve overall fluid flow and cell seeding efficiency within the channels. However, this approach is not without its caveats, as the size of a construct is limited by the depth of light penetration and the efficiency of photodegradation, which is dependent on the material properties and device set up [108]. A more standard approach to achieving interconnected multi-scale vasculature includes the generation of a EC-lined macroscale channel(s) embedded within a hydrogel consisting of co-culture of ECs and mural cells. This approach relies on spontaneous interconnections between ECs lining the channel and the self-assembled microvascular network inside the bulk hydrogel. This was demonstrated in an earlier study by Lee et al. who combined the principles of microfluidics and microvascular formation with the aim of constructing an interconnected system between macrovessels (lumen ~1 mm in diameter) and a self-assembled microvascular bed (Fig. 5D) [109]. As flow has been implicated in regulating angiogenesis, it was expected that perfusion of the macrovessels would promote angiogenic sprouting. Unexpectedly, it was found that continuous flow (shear stress: 10 dyn/cm^2) obstructed angiogenic sprouting into the matrix and was instead observed in static conditions, suggesting that the specific flow profile (magnitude, pulsatility, period of exposure) that they applied may not support angiogenic sprouting or even that flow may not be a requisite for angiogenic sprouting by itself [109]. However, once sprouting is achieved, flow within a system is still required in order to maintain the cell viability, drive cell maturation and lumen formation of the capillary plexus. This experimental finding suggests that it may be necessary to fine-tune the exposure to flow in a step-by-step manner with gradual increments of the flow in such a system [109]. Likely, *in vitro* mimicry of circumstances occurring during natural vasculogenesis, angiogenesis and plexus formation may be valuable in recapitulating such processes *in vitro*. Nevertheless, the study by Lee et al. provided early evidence that functional interconnections between EC-lined lumen and a capillary bed can be formed, albeit under static conditions. Building upon a similar strategy, Wang et al. introduced a larger-scale setup (7 mm diameter and 2 mm thick) consisting of a central diamond-shaped tissue chamber connected to two microfluidic channels on each end to represent an artery and vein (Fig. 5E-F) [110]. By introducing a VEGF gradient within the structure, and regulating medium viscosity and flow rate to achieve controlled laminar shear stresses in the range exhibited by native microvasculature (approximately 3 dyn cm^2), the group not only validated sprouting and anastomosis of the endothelialized channels with the surrounding self-assembled microcapillary network but also found the microscale vascular network to be functional and patent upon *in vitro* perfusion with minimal leakage [110].

In their seminal work, Miller and colleagues presented a highly flexible and automated fabrication strategy for creating vascularized tissue via sacrificial printing of sugar glass to generate interconnected tubular networks [46]. By introducing thermal extrusion and fiber drawing via a 3D printer, they were able to generate multi-scale vasculature comprising interconnected vessels of a range of diameters (150 to 800 µm) by simply manipulating the translational velocity of the extrusion nozzle, with inner diameters ranging from 800-1200 µm. The ECs introduced into the resulting lumina through a single inlet not only formed a continuous endothelium throughout the construct composed of varying vessel diameters but also exhibited single and multicellular sprouting from the vascular lumen and supported sustained metabolic function of cells embedded in the surrounding hydrogels at the core of volumetric constructs [46]. However, there are concerns surrounding the use of sugar glass as a fugitive ink with regard to the potential hyperglycemic cellular response following hydration of the lattice, highlighting the need for alternative biomaterials to create these multiscale templates. Taking *in vitro* approaches a step further, Szklanny et al. went beyond the *in vitro* characterizations of other studies and assessed the functionality of their novel biofabricated construct *in vivo* [111]. Using sacrificial molds, they first fabricated a polymeric tubular scaffold that was inserted into intercalated layers of cell-laden hydrogel printed with a dual head extrusion system, termed VascFold [111]. Upon cultivation, the fenestrations within the poly(l-lactide)-Poly(lactide-co-glycolide) (PLLA-PLGA) tubular scaffold permitted endothelial outgrowth into the hydrogel aspect of the scaffold. Next, as a pilot study to evaluate the functionality of VascFold *in vivo*, the construct was implanted to a rat femoral artery model. This direct anastomosis to the artery permitted immediate perfusion of blood through the construct (Fig. 5G-H). Remarkably, the construct displayed host vessel ingrowth into the fenestration after two weeks. The functionality of these α-SMA re-inforced vessels were confirmed via administration of a contrast agent which allowed visualization of the connection of vessels located in the surrounding hydrogel and the lumen of the polymeric scaffold. Within the hydrogel compartment, 3 different subgroups of vessels were identified ranging from small capillaries (<40 µm), intermediate vessels (40-60 µm) which resembled arteries and larger venule-like vessels (>60 µm). This novel approach which has the capacity to generate a hierarchical tree-like system could be used to vascularize a range of tissue engineered constructs, showing exciting advancements in the field of biofabrication.

In another study, Son et al. described a novel approach for fabricating a multi-scale microvasculature network by controlling angiogenic sprouting of a capillary network using angiogenic factor-secreting cells, i.e. normal human dermal fibroblasts (NHDFs). The research group first used sacrificial printing to generate endothelialized channels (≈800 µm width and 300 µm height). Next, the

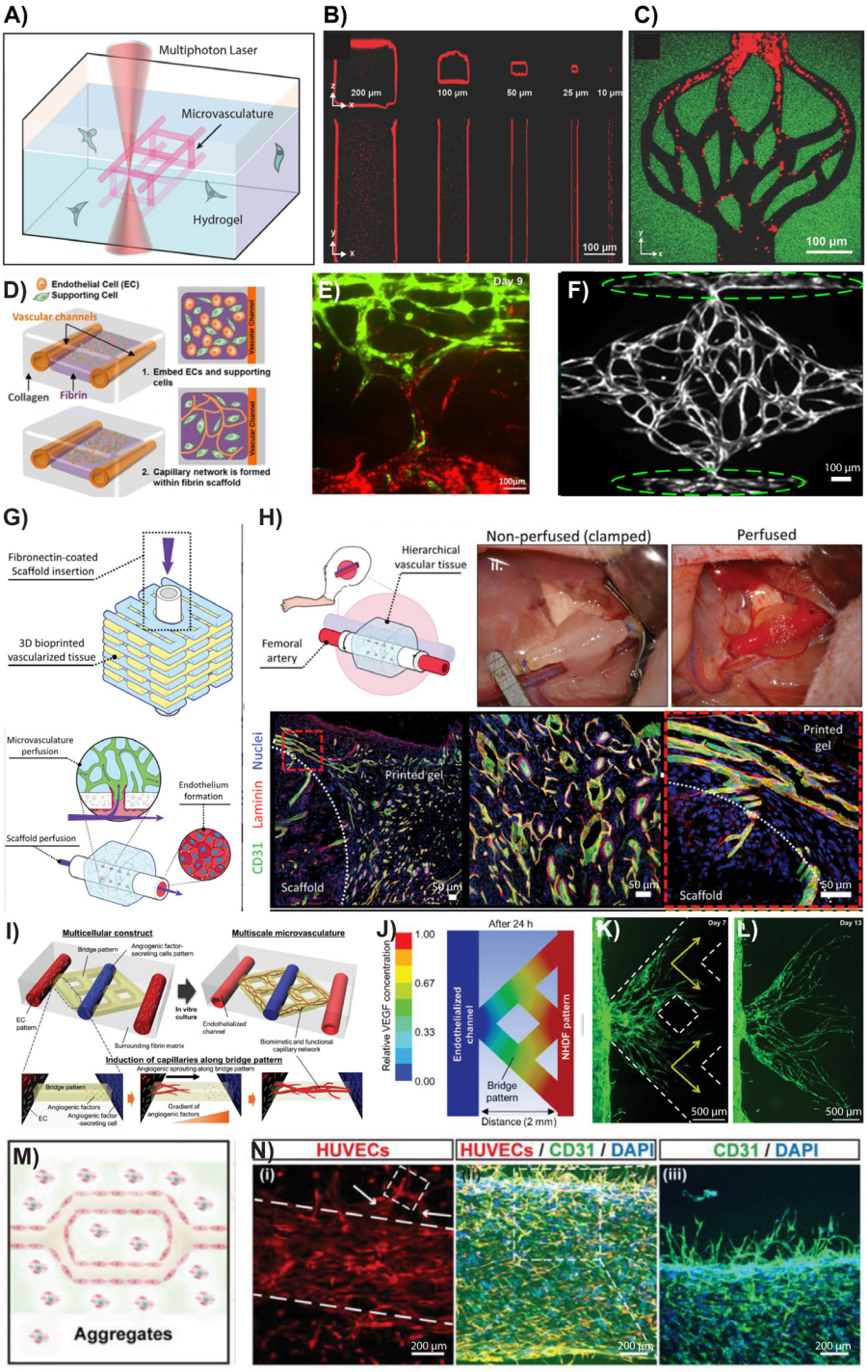

Fig. 5. Biofabrication approaches for the development of multi-scale, interconnected vascular structures. A) Graphical overview of multiphoton hydrogel photodegradation process. B) Resolution range of open, perfusable channels fabricated through multiphoton lithography and C) a multiscale vessel-like network fabricated in the same printing process; images reproduced with permission from [108]. D) Diagram of growth and maturation process of bioprinted multiscale vascular system and E) the resulting integration of the formed capillary network (green) with the sprouting major channels of the construct (red); images reproduced with permission from [109]. D) Complex, perfusable multiscale vessel network created through an anastomosed capillary bed with two larger channels; images reproduced with permission from [110]. G) Schematic of PLLA-PLGA VascFold fenestrated scaffold integrated into a EC-laden printed construct used to create an interconnected vessel network to support tissue growth and integration. H) After *in vitro* pre-culture of these scaffolds, implantation into a rat femoral artery model, the anastamosed implant was able to sustain perfusion *in vivo* and after two weeks, explanted tissues were highly vascularized as shown through laminin (red) and CD31 (green) stainings; images reproduced with permission from [111]. I) Schematic of multicellular construct to induce multiscale microvasculature composed of endothelialized channels and capillary network forming along bridging struts laden with NHDF cells that establish a pro-angiogenic growth factor gradient throughout the construct. J) Computer simulation of VEGF gradient established by NHDF cells. This growth factor gradient elicited capillary growth in a highly controlled spatial manner, showing branching into the different bridging struts after K) 7 and L) 13 days in culture; images reproduced with permission from [112]. M) Schematic diagram showing HUVEC and MSC coculture aggregates printed in a construct with a bifurcated central channel network. N) Fluorescence composite images displaying i): RFP–HUVECs seeded in printed channels. Arrows showing angiogenic HUVECs. Dotted box showing vascularized HUVEC aggregates. ii,iii): HUVECs expressed *CD31* attached in printed channels; images reproduced with permission from [113].

endothelialized channels were connected through a series of bridging cell-laden struts containing NHDF cells (Fig. 5I). The generated spatial gradient of angiogenic factors released from the NHDF cells were able to control the direction of angiogenic sprouting from the ECs lining the macrochannels (Fig. 5J-L). The interconnected microvessels had lumina of roughly 20 μm in diameter with a rough average sprout growth rate of 200 μm/day [112]. They verified the leak-free perfusability of their system via an *in vitro* perfusion system using fluorescently labelled dextran and an *ex vivo* chorioallantoic membrane (CAM) assay. The generated multi-scale vasculature was found to successfully integrate with host vasculature upon implantation with host blood perfused through the implanted capillary network showing another exciting development in the aim of creating an interconnected, multi-scale vascular network [112].

While the complexity and stability of printed bioinks have been vastly improved in recent years, most hydrogels are still not sufficiently mechanically robust to maintain long-term, open tubular structures as they are easily collapsible nor can they be anastomosed directly to a host vessel [51]. An example of how to overcome this problem, was reported by Liu et al. who incorporated an elastic hydrogel which imparted mechanical support to the macrovessel [113]. The bioprinted interconnected vascular structures were then surgically anastomosed to a carotid artery-to jugular-vein in a rat model. Upon implantation *in vivo*, the construct facilitated host vessel invasion into the surrounding graft with enhanced perfusion through the pre-generated vascular structures (Fig. 5M-N). However, the construct only survived 4 days post-implantation due too high hemodynamic pressures *in vivo*, indicating that further optimizations and improvements are still required for the model. Nevertheless, this study still serves as a stepping stone towards integrating hydrogel-based hollow vascular network with native vasculature and most certainly shows great strides in the right direction for the field [113].

3. Tissue engineering of vascularized bone constructs: current approaches, challenges and future perspectives

While significant improvements have been made in the field for the development of multiscale vasculature, a majority of the examples highlighted throughout this review are focused on standalone vascular structures, or are examples of applications for vascularizing soft tissues (e.g. liver). When it comes specifically to bone tissue engineering however, the combination of functional vascular and osteogenic components within a single construct has not been as widely reported in literature; likely due to the highly distinct biochemical and mechanical requirements each tissue possesses. From a mechanical standpoint, the fabrication of a prevascularized tissue engineered bone construct is complicated by the different biomechanical profiles needed to facilitate osteogenic and vascular growth. For example, in order to permit cellular migration and sprouting within a system, capillary networks typically require soft bulk matrices [114]. In contrast, osteogenic differentiation of progenitor cells is better supported by more rigid matrices [115]. For this reason, a majority of biofabrication approaches in bone tissue engineering have thus far relied on the body's intrinsic capacity for regeneration to achieve vascularization and bone ingrowth through methods such as manipulation of scaffold design [116–118] and/or use of bioactive composite scaffolds [119–122]. For instance, it has been shown that scaffolds consisting of large pores (>300 um) with a porosity of greater than 50% have superior angiogenic and osteogenic capacity *in vivo* [80]. However, as previously pointed out, in order to upscale to more clinically relevant sizes, a more sophisticated vascularization strategy needs to be adopted such as the (co)implantation of vascular and bone progenitor cells.

The process of bone formation is tightly intertwined with vasculogenesis, both during development and in the remodelling stage. Likewise, the success of bone regeneration and integration largely depends on adequate vascular supply for the delivery of nutrients, growth factors and hormones required by bone cells [123]. Thus, bone tissue engineering approaches that combine both osteogenic and vascular components are necessary in order to develop long-lasting functional grafts that are permissive for tissue regeneration. Both *in vitro* and *in vivo*, the indirect and direct cell-to-cell contact between MSCs and ECs has been reported to induce the differentiation of multipotent MSCs into a pericyte-like phenotype, which not only plays a role in the stabilization of the microvascular structures formed by the ECs but also aids in their maturation [124–126]. In the presence of osteogenic differentiation growth factors, multipotent MSCs can also differentiate into osteoblasts, mimicking the process of intramembranous ossification. The presence of osteoblasts is not only important for inducing osteogenesis, but also further reinforces the crosstalk with the ECs. For instance, formed osteoblasts secrete VEGF, which in turn promotes the expression of bone morphogenetic protein 2 (BMP-2) by ECs; thus creating a positive feedback loop that can be exploited for both osteogenesis and vasculogenesis to create a prevascularized engineered bone construct [127]. Capitalizing on this concept, a multitude of vasculogenic and osteogenic growth factors has been immobilized onto scaffolds to augment vascularization and bone formation. For the purpose of bone tissue engineering, this approach is particularly advantageous as multiple growth factors, which support angiogenesis and osteogenesis, can be immobilized onto a single scaffold. To mimic cellular processes *in vivo*, the release system of growth factors plays a pivotal role [128]. Multiple growth factors need to be delivered in a controlled and timely manner in order to recapitulate physiological signaling processes. Examples of growth factors with distinctive roles in vascular development include VEGF [129–131], fibroblast growth factor (FGF) [129,132,133] and platelet-derived growth factor (PDGF) [131,132] responsible for the recruitment of ECs, activation of EC proliferation and migration and maturation of blood vessels, respectively. In addition to the timely release, the 3D spatial arrangement of growth factors on or inside scaffolds that orchestrates vessel organization is seldom considered. The incorporation of distinct patterns of angiogenic growth factor gradients within a scaffold would permit improved spatial control over vascular organization. Recent technological advancements and improved understanding of bone development has enabled the delivery of angiogenic and osteogenic growth factors and genes with distinct spatiotemporal (release) profiles to improve bone regeneration [130,131,134]. An example of such an approach was demonstrated by Freeman et al. who utilized nanoparticle functionalized bioinks to fabricate implants with distinct growth factor patterns and release profiles to accelerate bone healing [130]. The coupling of a VEGF gradient with spatially defined BMP-2 localization led to improved bone formation *in vivo*, demonstrating the potential of spatiotemporally controlling the delivery of growth factors to concurrently enhance tissue specific maturation [130].

The application of biofabrication in bone tissue engineering would allow for the generation of complex tissues through the concomitant deposition of multiple bioinks with different mechanical properties within a single system to meet each the individual tissue requirements. Furthermore, as previously mentioned, different growth factors can be incorporated within each bioink to drive cell proliferation, differentiation and maturation. Current biofabrication approaches for vascularized bone tissue engineering can be divided into two categories, namely scaffold-free or scaffold-based approaches. Scaffold-free approaches typically rely on the self-assembly of ECs to form a microvascular network, mimicking the process of vascular development *in vivo* within an osteoinductive

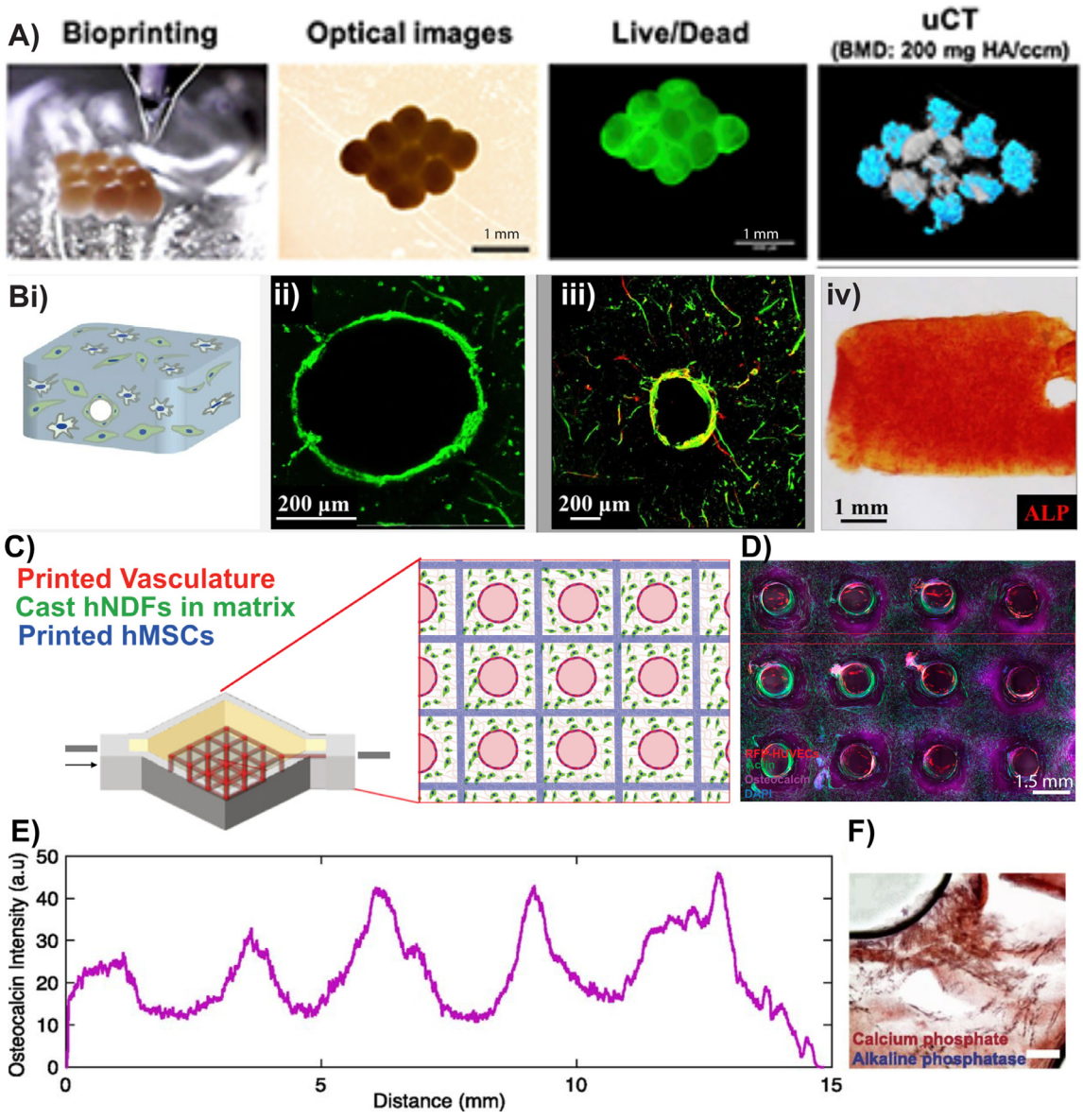

Fig. 6. Scaffold-free and scaffold-based approaches for vascularized bone tissue engineering. A) Process of aspiration-assisted bioprinting of HUVEC/MSC cell aggregates into a diamond architecture, depicting an optical image of the printed aggregates, LIVE/DEAD image to assess cell viability and a µCT scan showing bone formation and mineralization post-printing; images reproduced with permission from [135]. Bi) Graphical overview of pre-vascularized and osteogenically differentiated gelMA constructs, containing embedded ECFC-MSC co-cultures and a central channel seeded with ECFCs. ii) cross-section fluorescent image of the endothelialized channel and iii) a zoomed out image of the channel and surrounding embedded cells, showing sprouting between channel cells and the embedded co-cultures. iv) ALP-stained cross-section of the pre-vascularized, osteogenically differentiated construct showing alkaline phosphatase presence after 12 days of culture in optimized media; images reproduced with permission from [42]. C) Schematic of the printed heterogeneous tissue consisting of a sacrificial vascular network seeded with HUVECs, a printed hMSC lattice and casted NHDF within an ECM that fills the interstitial space. D) Confocal microscopy image through a cross-section of the thick vascularized osteogenic tissue construct after 30 d of active perfusion and in situ differentiation showing expression of osteocalcin in the printed and cast regions of the scaffold. E) Osteocalcin intensity across the thick tissue sample inside the red lines shown in D. F) Alizarin red staining of calcium phosphate deposition, and fast blue staining of alkaline phosphatases, indicating tissue maturation and differentiation over time; images reproduced with permission from [49].

environment. This approach takes advantage of cell-cell and cell-ECM interactions to closely mimic the native cellular environment required for vascularized bone tissue formation via the intramembranous route. This approach was reflected in a work by Heo et al. who generated vascularized bone tissue from spheroids consisting of human umbilical vein endothelial cells (HUVECs) and hMSCs using a bottom-up approach (Fig. 6A) [135]. Utilizing aspiration-assisted bioprinting (AAB), in which cellular aggregates are individually picked up through the application of negative pressure and patterned in a spatially controlled manner, they were able to precisely tailor the positioning of each spheroid without damaging these multicellular structures. After 10 days of osteogenic differentiation, spheroids of >500 µm in diameter containing HUVECs/hMSCs displayed enhanced osteogenesis and cell viability in the core in comparison to hMSC-only spheroids. However it is unclear if this was attributed to the shorter diffusion distances throughout the spheroids resulting from the emergence of vascular structures in the co-culture model or as a result of a more compact HUVECs/hMSCs spheroid in comparison to the hMSC-only spheroid resulting in enhanced diffusion. While the self-assembly of such small cellular units into distinct osteogenic and vascular structures is feasible to a certain extent (or dimension in this context), the generation of clinically relevant sized grafts that can be used in the clinic is extremely time consuming and cannot currently be

achieved without the development of high throughput manufacturing approaches. Furthermore, cellular self-assembly provides little spatial control over the orientation and 3D structure.

A more common and perhaps a more promising way to create a vascular network within bone tissue engineered constructs is through scaffold-based approaches in which a diverse range of biomaterials, from soft cell-supporting hydrogels to mechanically stabilizing polymers, can be precisely patterned to support and guide tissue architecture and function. Thus far, very limited studies have combined vascular and osteogenic culture within the same construct presumably due to the different nutrient requirement and physical environment required for each cell type, posing the question of how to achieve vascular and osteogenic co-cultures in a single *in vitro* system. This was eloquently addressed in a proof-of-concept set up by Klotz and colleagues who demonstrated the importance of modulating biomaterial properties and tailoring media composition to allow vascular and osteogenic growth in a single construct. By tuning the chemical properties of the widely used hydrogel GelMA, a permissive environment for vasculogenesis, angiogenic sprouting and migration, as well as osteogenic differentiation was created (Fig. 6B). The construct consisted of a central endothelialized macrovessel-like structure embedded within a co-culture of ECs and MSCs. Upon cultivation, vessel sprouting from the endothelialized channel connecting to the capillary-like structures inside the bulk hydrogel was observed, establishing of an interconnected multi-scale vessel network inside an osteogenic construct [42]. Such an approach demonstrated the feasibility of creating a multicellular tissue graft that possessed both osteogenic and angiogenic properties. In this classical tissue engineering approach however, the intricate bone architecture was not fully recapitulated, given the design limitations of conventional casting techniques. Nevertheless, the study highlighted the complexity of differentiating multiple cell types within a single system. In a previously discussed paper by Kolesky et al., the research group also showed the fabrication of a 10 cm^3 heterogeneous tissue architecture by simultaneously bioprinting a cell-laden gelatin-fibrinogen bioink loaded with MSCs and as fugitive ink Pluronic F-127, creating a branched vascular network [49]. The 3D symmetrical lattice channel network, with a single inlet and outlet, facilitated perfusion throughout the construct enabling nutrient and growth factor delivery into the core of the centimeter-scale tissue to enhance cell survival and to facilitate tissue differentiation (Fig. 6C) [49]. This study showed transvascular delivery of osteogenic differentiation media within a thick biofabricated tissue (Fig. 6D) [49]. Their results confirmed that their system facilitated growth factor delivery deep within the core of the construct as indicated by osteocalcin expression being proportional to the distance from the printed channels (Fig. 6E). Furthermore, these thick bioprinted constructs were maintained under constant perfusion for up to 30 days, thanks to the enhanced nutrient transport achieved through the patterned channels embedded in the prints, and displayed calcium phosphate and alkaline phosphatase production during this time (Fig. 6F) [49].

In recent years, there has also been a growing interest in mimicking endochondral ossification, the process of long bone formation where a transient cartilage template is remodelled into bone upon following vascular invasion [136–140]. In pursuit of recapitulating the intermediate stage of endochondral ossification, Nulty et al. proposed to prevascularize hypertrophic cartilage microtissues *in vitro* prior to implantation *in vivo* [136]. Using a microwell system, a large number of hypertrophic cartilage microtissues were generated from MSCs. Upon 5 weeks of differentiation, using a bottom-up approach, the microtissues were encapsulated within a fibrin-based hydrogel within PCL scaffold and prevascularized in a co-culture of HUVECs/MSCs for a week before implantation in an ectopic model. The prevascularized microtissues showed enhanced capacity to undergo mineralization *in vivo* after 4 weeks [136]. These cartilage microtissues could also be incorporated within a bioink and serve as building blocks that can be used to upscale bone tissue engineered constructs with pre-formed vascularized units.

Despite the promising developments in recent years in the creation of vasculature for bone tissue engineering, there are still several obstacles that must be considered and addressed before fully functional grafts can be generated for use in the clinic. From an engineering standpoint, the introduction of biofabrication approaches has greatly enhanced the size and complexity of tissue engineered constructs that can be created. As shown in this review, the use of different bioprinting technologies in combination with conventional tissue engineering strategies has allowed for the creation of multi-scale vascular networks that represent a major step in supporting long-term survival of tissue engineered constructs. However, these approaches still face important limitations for graft upscaling and maturation of native-like tissue functionality. While the introduction of a vascular network or template has been shown to increase the survival time of large bioprinted grafts (10 cm^3) [49], the architectural and multi-scale complexity of native vasculature has been difficult to recapitulate with a single fabrication approach alone. In recent years, researchers have proposed and began to explore the possibility of multitechnology biofabrication, in which the convergence of complementary bioprinting approaches could pose an answer to develop more advanced tissue engineered constructs and encompass a larger range of achievable resolutions and mechanical properties, as well as enhanced tissue-specific functionality [141]. For example, drop-on-demand (DoD) techniques have recently demonstrated the power of such convergence both in vitro and in vivo. Briefly, DoD approaches allow cellular aggregates of controllable sizes (including single cell resolutions) to be encapsulated in droplets of a biomaterial and precisely printed upon a substrate [142]. *In vitro*, these printed cellular aggregates have been shown to form hollow channels lined by a monolayer of ECs upon cellular self-assembly post-printing, reaching resolutions of up to 250 µm in fibrin/collagen substrates [143]. However, building complex 3D shapes using DoD is challenging given the difficulty in stacking multiple droplets on top of one another. Upon converging DoD techniques with extrusion-based bioprinting however, it is far more achievable to create complex, pre-vascularized scaffolds, by taking advantage of each technique's strengths. In this case, Rukavina et al., used extrusion bioprinting to create an adipose-derived stem cell (ASC)-laden bone mimic that would also serve to stabilize interspaced layers of DoD, self-assembling HUVEC aggregates in a fibrinogen gel that facilitated hollow channel formation within the stable bone-like construct. DoD drops of thrombin were also patterned next to the HUVEC aggregates to induce chemical crosslinking. Upon subcutaneous implantation in immunodeficient mice, extensive matrix calcifation was observed within the construct after 12 days, and vessels with lumens ranging from 9-190 µm were formed, supported by mouse-derived mural cells, suggesting integration with the mouse tissue at the implant site [144]. Such studies demonstrate the advantages of converging different bioprinting strategies with differing strengths and limitations and bring about great promise for future developments using the many techniques discussed throughout this review. When looking at the potential for clinical translation of current biofabricated constructs however, other concerns arise. Critically, the fabrication times of large and convoluted structures needed to repair critical tissue defects are extremely time consuming. The layer-by-layer fabrication approach employed by most bioprinting strategies to date means that increasing the size of printed constructs results in a significantly longer printing times, during which cells are subjected to suboptimal conditions. Given that processing times of just 30 minutes can lead to detrimental effects in cell metabolism [145], this

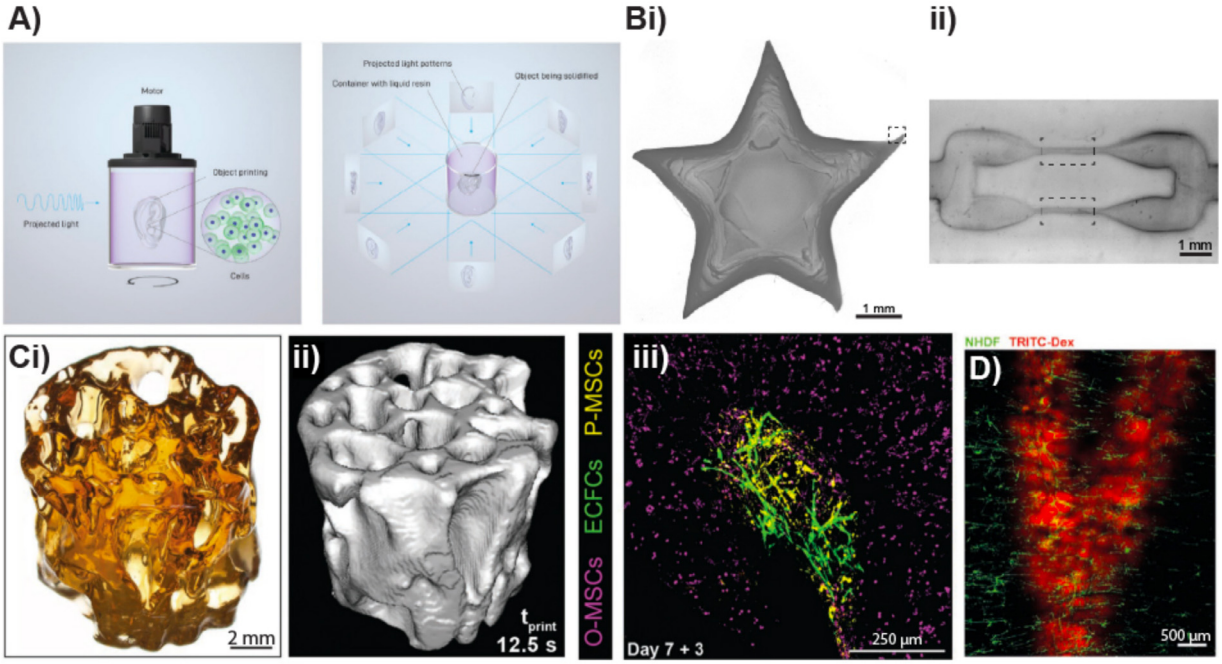

Fig. 7. Volumetric bioprinting as a promising approach for creating large-scale vascularized constructs at high speeds. A) Graphical overview of the volumetric bioprinting process, in which visible light projections are orchestrated towards a light-sensitive resin and elicit a one-step polymerization approach to create large constructs within seconds; images reproduced with permission from [146]. B) Recent developments of this technique allow for high resolution of positive (~40 µm) and negative (~100 µm) features; images reproduced with permission from [148]. Ci) Digital image and ii) µCT reconstruction of an anatomical trabecular bone model printed via VBP, iii) 3 days after seeding the pores of the printed structure with ECs and MSCs angiogenic sprouting was observed;; images reproduced with permission from [146]. D) Bifurcated channel structure printed with a mechanically tunable hydrogel (gelatin norbornene) using VBP; images reproduced with permission from [149].

means that creating large-scale constructs of clinical relevance in the range of cubic centimeters (1-10 cm^3 for large bone defects) could result in significantly hampered cellular activity and would likely impair optimal function upon implantation. While steps can be taken to ensure physiological temperatures and oxygen levels can be matched inside the printer, to guarantee that all cells and materials are homogenously exposed to these factors remains a challenge, and may result in different cellular responses throughout a construct printed over time.

Recently, a novel optical tomography-inspired bioprinting approach has come to light that brings a paradigm-shift to conventional bioprinting methodology and could be the key to overcome the upscaling and design limitations from past bioprinting studies [146]. Volumetric printing is a light-based, single-step printing approach, in which tomographic light projections are directed towards a light-sensitive polymer and lead to the formation of a 3D object within tens of seconds (Fig. 7A) [147]. This layer-less approach has been used for the ultrafast volumetric bioprinting (VBP) of biocompatible hydrogels, proving to support cell survival and function, while allowing for high accuracy printing of anatomical structures. Recently, positive features of ~40 µm and open channels of ~100 µm in diameter have been achieved, showing great promise for the development of higher resolution vascularized constructs (Fig. 7B) [146,148]. In a study introducing VBP for tissue engineering applications, an anatomical model of equine trabecular bone with positive features in the range of 140 µm was successfully printed, showing a complex, interconnected pore network (Fig. 7Ci-ii) [146]. When ECs were seeded inside the open pores of the printed bone structure, angiogenic sprouting into the printed osteogenic compartment was observed within three days (Fig. 7Ciii). Given the single-step nature of this printing approach, constructs of up to 4.14 cm^3 have been obtained within tens of seconds, thus taking an important step in the upscaling capabilities of such a printing approach [146]. Research on VBP has also elucidated the potential for engineering large-scale perfusable grafts using mechanically tunable biomaterials (Fig. 7D) [149]. The possibility to print out-of-plane, highly convoluted vessel networks is also enhanced by the design freedom offered by the layer-less nature of VBP. Despite the promising advantages of VBP in the development of large-scale convoluted constructs and given the young age of this technique, some work remains to be done regarding the printing resolution needed to create an anatomically-scaled vascular network that includes the high-resolution microcapillary structures essential for efficient vascularization of tissue models. Furthermore, given that this technology is still in its infancy, a broader range of biomaterials and combination of cell types will need to be evaluated for use in VBP, in order to advance this technique and to ensure clinical translatability is possible in the future. The incorporation of different materials, inductive for distinct target tissues, and multiple cell types in the same printed construct using this ultra-fast technique could open doors to create more intricate vascularized bone implants in coming years.

4. Conclusion

One of the most arduous challenges in upscaling the size of engineered bone tissue to clinically relevant sizes has undoubtedly been the lack of an integrated vascular network. As an engineered construct exceeds the diffusional limit, a vascular network is required for the delivery of nutrients to cells and in the case of bone tissue engineering, to drive differentiation of cells in the bulk matrix during the construct's maturation process. The engineered network should be able to connect to the host vasculature system upon implantation, ideally via microsurgical anastomosis to allow for immediate perfusion throughout the construct. In recent decades, significant technological advancements, particularly in the field of biofabrication have brought about impressive progress and encouraging steps towards engineering complex vascular networks. Continuous improvements in resolutions and ever-increasing freedom of design offered by different bioprinting ap-

proaches discussed above have enabled the generation of vascular channels of diameters ranging from the centimeter down to the micrometer scale. However, while current technologies have been able to tackle different scales of the vascular tree, only a handful of studies highlighted in this review have demonstrated the capability to print and perfuse a multi-scale, interconnected standalone vascular network.

Furthermore, integrating such a complex vascular network to bone tissue engineered constructs poses additional biological and technological challenges given the two tissue's distinct biomechanical requirements. Thus far, very few studies have used an integrated approach to create an osteogenically differentiated tissue engineered construct composed of multiscale vasculature. In order to recapitulate the cellular organisation of native bone tissues, it is clear that multiple biofabrication approaches need to be combined into one unified multi-faceted approach. Another promising approach is VBP, a game changer in the field which overcomes several limitations associated with traditional 3D printing in terms of design freedom and more importantly printing time. In this review, we have highlighted some of the key technological advancements which have the potential to drive the field forward and breakdown existing barriers in order to achieve the ultimate goal of biofabricating the vascular tree in engineered bone. As both the versatility of fabrication technologies and our understanding of (vascular) biology progress to address these open challenges, huge progress could be expected in the realization of a vascularized tissue engineered bone construct that can be reliably implanted and reach clinical relevance for the field of regenerative medicine. Despite the many advancements discussed in this review, there is still a long way to go before this technology becomes common practice. However, if the development of technological advancements continues at the current rate, the feasibility of creating a functional bone tissue engineered construct may be within the bounds of possibility in the near future.

Declaration of Competing Interest

The authors declare that they have no known competing financial interests or personal relationships that could have appeared to influence the work reported in this paper.

Acknowledgements

This work was supported by the Marie Skłodowska-Curie Actions (Grant agreement RESCUE #801540), European Research Council (ERC) under the European Union's Horizon 2020 research and innovation programme (grant agreement No. 949806, VOLUME-BIO), European's Union's Horizon 2020 research and innovation programme under grant agreement No 964497 (ENLIGHT), ReumaNederland (LLP-12, LLP22, and 19-1-207 MINIJOINT) and the Gravitation Program "Materials Driven Regeneration", funded by the Netherlands Organization for Scientific Research (024.003.013).

References

[1] A.H. Schmidt, Autologous bone graft: Is it still the gold standard? Injury 52 (2021) S18–S22.
[2] A. Oryan, S. Alidadi, A. Moshiri, N. Maffulli, Bone regenerative medicine: classic options, novel strategies, and future directions, J. Orthop. Surg. Res. 9 (1) (2014) 18.
[3] R. Agarwal, A.J. García, Biomaterial strategies for engineering implants for enhanced osseointegration and bone repair, Adv. Drug. Deliv. Rev. 94 (2015) 53–62.
[4] L. Roseti, V. Parisi, M. Petratta, C. Cavallo, G. Desando, I. Bartolotti, B. Grigolo, Scaffolds for bone tissue engineering: state of the art and new perspectives, Mater. Sci. Eng. C Mater. Biol. Appl. 78 (2017) 1246–1262.
[5] A.R. Amini, C.T. Laurencin, S.P. Nukavarapu, Bone tissue engineering: recent advances and challenges, Crit. Rev. Biomed. Eng. 40 (5) (2013) 363–408.
[6] Á.E. Mercado-Pagán, M. Stahl, Y. Shanjani, Y. Yang, Vascularization in bone tissue engineering constructs, Ann. Biomed. Eng. 43 (3) (2015) 718–729.
[7] S. Bhumiratana, G. Vunjak-Novakovic, Concise review: personalized human bone grafts for reconstructing head and face, Stem Cells Transl. Med. 1 (1) (2012) 64–69.
[8] J.R. Perez, D. Kouroupis, D.J. Li, T.M. Best, L. Kaplan, D. Correa, Tissue engineering and cell-based therapies for fractures and bone defects, Front. Bioeng. Biotechnol. 6 (2018) 105.
[9] v.B.C. A. H. Yuan, H. Fernandes, P. Hobibovic, J. de Boer, A.M.C. Barradas, A. de Ruiter, W.R. Walsh, J.D. de Bruijn, Osteoinductive ceramics as a synthetic alternative to autologous bone grafting, Proc. Natl. Acad. Sci. U. S. A. 107 (31) (2010) 13614–13619.
[10] D. T. Zhu, T. Cui, M.Z. Zhang, J. Ding, Engineered three-dimensional scaffolds for enhanced bone regeneration in osteonecrosis, Bioact. Mater. 5 (3) (2020) 584–601.
[11] J.A. Fialkov, C.E. Holy, M.S. Shoichet, J.E. Davies, In vivo bone engineering in a rabbit femur, J. Craniomaxillofac. Surg. 14 (3) (2003) 324–332.
[12] S.P. Bruder, K.H. Kraus, V.M. Goldberg, S. Kadiyala, The effect of implants loaded with autologous mesenchymal stem cells on the healing of canine segmental bone defects, J. Bone. Joint Surg. Am. 80 (7) (1998) 985–996.
[13] Y. He, Z.Y. Zhang, H.G. Zhu, W. Qiu, X. Jiang, W. Guo, Experimental study on reconstruction of segmental mandible defects using tissue engineered bone combined bone marrow stromal cells with three-dimensional tricalcium phosphate, J. Craniofac. Surg. 18 (4) (2007) 800–805.
[14] H. Abukawa, M. Shin, W.B. Williams, J.P. Vacanti, L.B. Kaban, M.J. Troulis, Reconstruction of mandibular defects with autologous tissue-engineered bone, J. Oral Maxillofac. Surg. 62 (5) (2004) 601–606.
[15] H. Petite, V. Viateau, W. Bensaïd, A. Meunier, C. de Pollak, M. Bourguignon, K. Oudina, L. Sedel, G. Guillemin, Tissue-engineered bone regeneration, Nat. Biotechnol. 18 (9) (2000) 959–963.
[16] H. Schliephake, J.W. Knebel, M. Aufderheide, M. Tauscher, Use of cultivated osteoprogenitor cells to increase bone formation in segmental mandibular defects: an experimental pilot study in sheep, Int. J. Oral Maxillofac. Surg. 30 (6) (2001) 531–537.
[17] L. Zhu, W. Liu, L. Cui, Y. Cao, Tissue-engineered bone repair of goat-femur defects with osteogenically induced bone marrow stromal cells, Tissue Eng. 12 (3) (2006) 423–433.
[18] G.S. Liu, L. Zhao, W. Zhang, L. Cui, W. Liu, Y. Cao, Repair of goat tibial defects with bone marrow stromal cells and β-tricalcium phosphate, J. Mater. Sci. Mater. Med. 19 (6) (2008) 2367–2376.
[19] J. Rouwkema, B. Koopman, C. Blitterswijk, W. Dhert, J. Malda, Supply of nutrients to cells in engineered tissues, Biotechnol. Genet. Eng. Rev. 26 (2010) 163–178.
[20] F. Simunovic, G. Finkenzeller, Vascularization strategies in bone tissue engineering, Cells 10 (7) (2021) 1749.
[21] P. Carmeliet, R.K. Jain, Angiogenesis in cancer and other diseases, Nature 407 (6801) (2000) 249–257.
[22] R.K. Jain, P. Au, J. Tam, D.G. Duda, D. Fukurama, Engineering vascularized tissue, Nature Biotechnol. 23 (2005) 821–823.
[23] Y. Du, M. Ghodousi, H. Qi, N. Haas, W. Xiao, A. Khademhosseini, Sequential assembly of cell-laden hydrogel constructs to engineer vascular-like microchannels, Biotechnol. Bioeng. 108 (7) (2011) 1693–1703.
[24] Y. Zhang, N. Fisher, S.E. Newey, J. Smythe, L. Tatton, G. Tsaknakis, S.P. Forde, L. Carpenter, T. Athanasspoulos, S.J. Hale, D.J. Ferguson, M.P. Tyler, S.M. Watt, The impact of proliferative potential of umbilical cord-derived endothelial progenitor cells and hypoxia on vascular tubule formation in vitro, Stem Cells Dev. 18 (2) (2009) 359–375.
[25] S. Shafiee, S. Shariatzadeh, A. Zafari, A. Majd, H. Niknejad, Recent advances on cell-based co-culture strategies for prevascularization in tissue engineering, Front. Bioeng. Biotechnol. 9 (745314) (2021).
[26] Y. Kang, S. Kim, M. Fahrenholtz, A. Khademhosseini, Y. Yang, Osteogenic and angiogenic potentials of monocultured and co-cultured human-bone-marrow-derived mesenchymal stem cells and human-umbilical-vein endothelial cells on three-dimensional porous beta-tricalcium phosphate scaffold, Acta Biomater. 9 (1) (2013) 4906–4915.
[27] N. Koike, D. Fukurama, O. Gralla, P. Au, J.S. Schechner, R.K. Jain, Creation of long-lasting blood vessels, Nature 428 (2004) 138–198.
[28] F. Kawecki, T. Galbraith, W.P. Clafshenkel, M. Fortin, F.A. Auger, J. Fradette, In vitro prevascularization of self-assembled human bone-like tissues and preclinical assessment using a rat calvarial bone defect model, Materials (Basel) 14 (8) (2021) 2023.
[29] M.A. Kuss, S. Wu, Y. Wang, J.B. Untrauer, W. Li, J.Y. Lim, B. Duan, Prevascularization of 3D printed bone scaffolds by bioactive hydrogels and cell co-culture, J. Biomed. Mater. Res. B Appl. Biomater. 106 (5) (2018) 1788–1798.
[30] R. Subbiah, G. Thrivikraman, S.P. Parthiban, J.M. Jones, A. Athirasala, H. Xie, L.E. Bertassoni, Prevascularized hydrogels with mature vascular networks promote the regeneration of critical-size calvarial bone defects in vivo, J. Tissue Eng. Regen. Med. 15 (3) (2021) 219–231.
[31] R. Mishra, B.M. Roux, M. Posukonis, E. Bodamer, E.M. Brey, J.P. Fisher, D. Dean, Effect of prevascularization on in vivo vascularization of poly(propylene fumarate)/fibrin scaffolds, Biomaterials 77 (2016) 255–266.
[32] M. Sladkova, G.M. De Peppo, Bioreactor Syst. Human Bone Tissue Eng. Process. 2 (2014) 494–525.
[33] A.S. Goldstein, T.M. Juarez, C.D. Helmke, M.C. Gustin, A.G. Mikos, Effect of convection on osteoblastic cell growth and function in biodegradable polymer foam scaffolds, Biomaterials 22 (11) (2001) 1279–1288.

[34] J. Groll, T. Boland, T. Blunk, J.A. Burdick, D.-W.W. Cho, P.D. Dalton, B. Derby, G. Forgacs, Q. Li, V.A. Mironov, L. Moroni, M. Nakamura, W. Shu, S. Takeuchi, G. Vozzi, T.B.F.F. Woodfield, T. Xu, J.J. Yoo, J. Malda, Biofabrication: reappraising the definition of an evolving field, Biofabrication 8 (2016) 013001.
[35] W.S. Harley, C.C. Li, J. Toombs, C.D. O'Connell, H.K. Taylor, D.E. Heath, D.J. Collins, Advances in biofabrication techniques towards functional bioprinted heterogeneous engineered tissues: a comprehensive review, Bioprinting 23 (2021) e00147.
[36] R. Levato, T. Jungst, R.G. Scheuring, T. Blunk, J. Groll, J. Malda, From shape to function: the next step in bioprinting, Adv. Mater. 32 (12) (2020) 1906423.
[37] C. Spadaccio, A. Rainer, R. Barbato, M. Trombetta, M. Chello, B. Meyns, The long-term follow-up of large-diameter Dacron® vascular grafts in surgical practice: a review, J. Cardiovasc. Surg. (Torino) 60 (4) (2019) 501–513.
[38] P. Mallis, A. Kostakis, C. Stavropoulos-Giokas, E. Michalopoulis, Future perspectives in small-diameter vascular graft, Bioengineering (Basel) 7 (4) (2020) 160.
[39] Y. Matsuzaki, K. John, T. Shoji, T. Shinoka, The Evolution of Tissue Engineered Vascular Graft Technologies: From Preclinical Trials to Advancing Patient Care, Appl Sci (Basel 9 (7) (2019) 1274.
[40] A. Weekes, N. Bartnikowski, N. Pinto, J. Jenkins, C. Meinert, T.J. Klein, Biofabrication of small diameter tissue-engineered vascular grafts. 138, 2022: p. 92-111.
[41] T. Takei, S. Sakai, T. Ono, H. Ijima, K. Kawakami, Fabrication of endothelialized tube in collagen gel as starting point for self-developing capillary-like network to construct three-dimensional organs in vitro, Biotechnol. Bioeng. 95 (1) (2006) 1–7.
[42] B. Klotz, K.S. Lim, Y.X. Chang, B.G. Soliman, I. Pennings, F.P.W. Melchels, T.B.F. Woodfield, A.J.W.P. Rosenberg, J. Malda, D. Gawlitta, Engineering of a complex bone tissue model with endothelialised channels and capillary-like networks, Eur. Cell Mater. 35 (2018) 335–348.
[43] K.M. Chrobak, D.R. Potter, J. Tien, Formation of perfused, functional microvascular tubes in vitro, Microvasc. Res. 71 (3) (2006) 185–196.
[44] T. Neumann, B.S. Nicholson, J.E. Sanders, Tissue engineering of perfused microvessels, Microvasc. Res. 66 (1) (2003) 59–67.
[45] J. Hammer, L.H. Han, X. Tong, F. Yang, A facile method to fabricate hydrogels with microchannel-like porosity for tissue engineering, Tissue Eng. Part C Methods 20 (2) (2014) 169–176.
[46] J.S. Miller, K.R. Stevens, M.T. Yang, B.M. Baker, D.T. Nguyen, D.M. Cohen, E. Toro, A.A. Chen, P.A. Galie, X. Yu, R. Chaturvedi, S.N. Bhatia, C.S. Chen, Rapid casting of patterned vascular networks for perfusable engineered three-dimensional tissues, Nat. Med. 11 (9) (2012) 768–774.
[47] L.S. W. X.Y. Wang, Z.H. Jin, B.W. Gan, M. Xie, W.H. Huang, Engineering interconnected 3D vascular networks in hydrogels using molded sodium alginate lattice as the sacrificial template, Lab Chip 14 (15) (2014) 2709.
[48] W. Wu, C.J. Hansen, A.M. Aragón, P.H. Geubelle, S.R. White, J.A. Lewis, Direct-write assembly of biomimetic microvascular networks for efficient fluid transport, Soft Matter. 6 (4) (2010) 739–742.
[49] D.B. Kolesky, K.A. Homan, M. Skylar-Scott, J.A. Lewis, Three-dimensional bioprinting of thick vascularized tissues, PNAS 113 (12) (2016) 3179–3184.
[50] L. Ouyang, J.P.K. Armstrong, Q. Chen, Y. Lin, M.M. Stevens, Void-Free 3D bioprinting for in situ endothelialization and microfluidic perfusion, Adv. Funct. Mater. 30 (1) (2020) 1908349.
[51] L. Shao, Q. Gao, J. Fu, M. Xiang, Y. He, Directly coaxial 3D bioprinting of large-scale vascularized tissue constructs, Biofabrication 12 (3) (2020) 035014.
[52] A. Schwab, R. Levato, M. D'Este, S. Piluso, D. Eglin, J. Malda, Printability and shape fidelity of bioinks in 3D bioprinting, Chem. Rev. 120 (19) (2020) 11028–11055.
[53] A. Ribeiro, M.M. Blokzijl, R. Levato, C.W. Visser, M. Castilho, W.E. Hennink, T. Vermonden, J. Malda, Assessing bioink shape fidelity to aid material development in 3D bioprinting, Biofabrication 10 (1) (2017) 014102.
[54] J.T. Muth, D.M. Vogt, R.L. Truby, Y. Mengüç, D.B. Kolesky, R.J. Wood, J.A. Lewis, Embedded 3D printing of strain sensors within highly stretchable elastomers, Adv. Mater. 26 (36) (2014) 6307–6312.
[55] T.J. sky, Q. Jallerat, R.N. Palchesko, J.H. Park, M.S. Grodzicki, H.-J. Shue, M.H. Ramadan, A.R. Hudson, A.W. Feinberg, Three-dimensional printing of complex biologicalstructures by freeform reversible embedding ofsuspended hydrogels, Sci. Adv. 1 (9) (2015) e1500758.
[56] H. Savoji, L.D. Huyer, M.H. Mohammadi, B.F.L. Lai, N. Rafatian, D. Bannerman, M. Shoaib, E.R. Bobicki, A. Ramachandran, M. Radisic, 3D printing of vascular tubes using bioelastomer prepolymers by freeform reversible embedding, ACS Biomater. Sci. Eng. 6 (3) (2020) 1333–1343.
[57] M. Skylar-Scott, S.G.M. Uzel, L.L. Nam, J.H. Ahrens, R.L. Truby, Biomanufacturing of organ-specific tissues with high cellular density and embedded vascular channels, Sci. Adv. 5 (9) (2019) eaaw2459.
[58] C. Dikyol, M. Altunbek, B. Koc, Embedded multimaterial bioprinting platform for biofabrication of biomimetic vascular structures, J. Mater. Res. 36 (2021) 3851–3864.
[59] F. Koch, K. Tröndle, G. Finkenzeller, R. Zengerle, S. Zimmermann, P. Koltay, Generic method of printing window adjustment for extrusion-based 3D-bioprinting to maintain high viability of mesenchymal stem cells in an alginate-gelatin hydrogel, Bioprinting 20 (2020) e00094.
[60] T. Jungst, W. Smolan, K. Schacht, T. Scheibel, J. Groll, Strategies and molecular design criteria for 3D printable hydrogels, Chem. Rev. 116 (3) (2016) 1496–1539.
[61] M. Lee, R. Rizzo, F. Surman, M. Zenobi-Wong, Guiding lights: tissue bioprinting using photoactivated materials guiding lights: tissue bioprinting using photoactivated materials, Chem. Rev. 120 (19) (2020) 10950–11027.
[62] K.S. Lim, B.S. Schon, N.V. Mekhileri, G.C.J. Brown, C.M. Chia, S. Prabakar, G.J. Hooper, T.B.F. Woodfield, New visible-light photoinitiating system for improved print fidelity in gelatin-based bioinks, ACS Biomater. Sci. Eng. 2 (10) (2016) 1752–1762.
[63] J. Dahle, E. Kvam, T. Stokke, Bystander effects in UV-induced genomic instability: antioxidants inhibit delayed mutagenesis induced by ultraviolet A and B radiation, J. Carcinog. 4 (2005) 11.
[64] J. Zhang, Q. Hu, S. Wang, J. Tao, M. Gou, Digital light processing based three-dimensional printing for medical applications, Int. J. Bioprint 6 (1) (2020) 242.
[65] E.R. Ruskowitz, C.A. DeForest, Proteome-wide analysis of cellular response to ultraviolet light for biomaterial synthesis and modification, ACS Biomater. Sci. Eng. 5 (5) (2019) 2111–2116.
[66] R. Zhang, N.B. Larsen, Stereolithographic hydrogel printing of 3D culture chips with biofunctionalized complex 3D perfusion networks, Lab Chip 17 (24) (2017) 4273–4282.
[67] R. Levato, K.S. Lim, W. Li, A.U. Asua, L.B. Peña, M. Wang, M. Falandt, P.N. Bernal, D. Gawlitta, Y.S. Zhang, T.B.F. Woodfield, J. Malda, High-resolution lithographic biofabrication of hydrogels with complex microchannels from low-temperature-soluble gelatin bioresin, Mater. Today Bio. 12 (2021) 100162.
[68] B. Grigoryan, S.J. Paulsen, D.C. Corbett, D.W. Sazer, C.L. Fortin, A.J. Zaita, P.T. Greenfield, N.J. Calafat, J.P. Gounley, A.H. Ta, F. Johansson, A. Randles, J.E. Rosenkrantz, J.D. Louis-Rosenberg, P.A. Galie, K.R. Stevens, J.S. Miller, Multivascular networks and functional intravascular topologies within biocompatible hydrogels, Science 364 (6439) (2019) 458–464.
[69] X. Ma, X. Qu, W. Zhu, Y.-S. Li, S. Yuan, H. Zhang, J. Liu, P. Wang, C.S.E. Lai, F. Zanella, G.-S. Feng, F. Sheikh, S. Chien, S. Chen, Deterministically patterned biomimetic human iPSC-derived hepatic model via rapid 3D bioprinting, Proc. Nat. Acad. Sci. 113 (8) (2016) 2206–2211.
[70] W. Zhu, X. Qu, J. Zhu, X. Ma, S. Patel, J. Liu, P. Wang, C.S.E. Lai, M. Gou, Y. Xu, K. Zhang, S. Chen, Direct 3D bioprinting of prevascularized tissue constructs with complex microarchitecture, Biomaterials 124 (2017) 106–115.
[71] K.S. Lim, R. Levato, P.F. Costa, M. Castilho, C.R. Alcala-Orozco, L.H.A. van Dommelen, F.P.W. Melchels, D. Gawlitta, G.J. Hooper, J. Malda, T.B.F. Woodfield, Bio-resin for high resolution lithography-based biofabrication of complex cell-laden constructs, Biofabrication 10 (3) (2018) 034101.
[72] O.C. Cassell, S.O.P. Hofer, K.R. Knight, Vascularisation of tissue-engineered grafts: the regulation of angiogenesis in reconstructive surgery and in disease states, Br. J. Plast. Surg. 55 (8) (2002) 603–610.
[73] R.R. Chen, E.A. Silva, W.W. Yuen, D.J. Mooney, Spatio-temporal VEGF and PDGF delivery patterns blood vessel formation and maturation, Pharm. Res. 24 (2) (2007) 258–264.
[74] S. Wang, F. Umrath, W. Cen, S. Reinert, D. Alexander, Angiogenic potential of VEGF mimetic peptides for the biofunctionalization of collagen/hydroxyapatite composites, Biomolecules 11 (10) (2021) 1358.
[75] N.J. Shah, M.L. Macdonalds, Y.M. Beben, R.F. Padera, R.E. Samuel, P.T. Hammond, Tunable dual growth factor delivery from polyelectrolyte multilayerfilms, Biomaterials 32 (26) (2011) 6183–6193.
[76] P.A. Turner, J.S. Thiele, J.P. Stegemann, Growth factor sequestration and enzyme-mediated release from genipin-crosslinked gelatin microspheres, J. Biomater. Sci. Polym. Ed. 28 (16) (2017) 1826–1846.
[77] A. Stejskalová, F.J. England, B.D. Almquist, Biologically inspired, cell-selective release of aptamer-trapped growth factors by traction forces, Adv. Mater. 31 (7) (2019) 1806380.
[78] L.R. Madden, D.J. Mortisen, E.M. Sussman, S.K. Dupras, J.A. Fugate, J.L. Cuy, K.D. Hauch, M.A. Laflamme, C.E. Murry, B.D. Ratner, Proangiogenic scaffolds as functional templates for cardiac tissue engineering, Proc. Natl. Acad. Sci. U S A, 107 (34) (2010) 15211–15216.
[79] S.A. Biela, Y. Su, J.P. Spatz, R. Kemkemer, Different sensitivity of human endothelial cells, smooth muscle cells and fibroblasts to topography in the nano–micro range, Acta Biomater. 5 (7) (2009) 2460–2466.
[80] V. Karageorgiou, D. Kaplan, Porosity of 3D biomaterial scaffolds and osteogenesis, Biomaterials 26 (27) (2005) 5474–5491.
[81] M.F.A. Cutiongco, S.H. Goh, R. Aid-Launais, C.L. Visage, H.Y. Low, E.K.F. Yim, Planar and tubular patterning of micro and nano-topographies on poly(vinyl alcohol) hydrogel for improved endothelial cell responses, Biomaterials 84 (2016) 184–195.
[82] Y. Chen, S. Chen, N. Kawazoe, G. Chen, Promoted angiogenesis and osteogenesis by dexamethasone-loaded calcium phosphate nanoparticles/collagen composite scaffolds with microgroove networks, Sci. Rep. 8 (1) (2018) 14143.
[83] T. Yu, C. Dong, Z. Shen, Y. CHen, B. Yu, H. Shi, C. Zhou, J. Ye, Vascularization of plastic calcium phosphate cement in vivo induced by in-situ-generated hollow channels, Mater. Sci. Eng. C Mater. Biol. Appl. 68 (2016) 153–162.
[84] F.E. Freeman, D.C. Browe, J. Nulty, S.V. Euw, W.L. Grayson, D.J. Kelly, Biofabrication of multiscale bone extracellular matrix scaffolds for bone tissue engineering, Eur. Cell Mater. 38 (2019) 168–187.
[85] U. Utzinger, B. Bagget, J.A. Weiss, J.B. Hoying, L.T. Edgar, Large-scale time series microscopy of neovessel growth during angiogenesis, Angiogenesis 18 (3) (2015) 219–232.
[86] T. Maciag, J. Kadish, L. Wilkins, M.B. Stemerman, R. Weinstein, Organizational behavior of human umbilical vein endothelial cells, J. Cell Biol. 94 (3) (1982) 511–520.
[87] J. Folkman, C. Haudenschild, Angiogenesis in vitro, Nature 288 (1980) 551–556.

[88] R. Montesano, L. Orci, P. Vassalli, In vitro rapid organization of endothelial cells into capillary-like networks is promoted by collagen matrices, J. Cell Biol. 97 (5) (1983) 1648–1652.
[89] J.A. Madri, S.K. Williams, Capillary endothelial cell cultures: phenotypic modulation by matrix components, J. Cell Biol. 97 (1) (1983) 153–165.
[90] J.M. Melero-Martin, M.E. De Obaldia, S.-Y. Kang, Z.A. Khan, L. Yuan, P. Oettgen, J. Bischoff, Engineering robust and functional vascular networks in vivo with human adult and cord blood–derived progenitor cells, Circulat. Res. 103 (2) (2008) 194–202.
[91] A. Khademhosseini, R. Langer, J. Borenstein, J.P. Vacanti, Microscale technologies for tissue engineering and biology, Proc. Natl. Acad. Sci. U S A, 103 (8) (2006) 2480–2487.
[92] J. Borenstein, H. Terai, K.R. King, E.J. Weinberg, M.R. Kaazempur-Mofrad, J.P. Vacanti, Microfabrication technology for vascularized tissue engineering, Biomed. Microdevices 4 (2002) 167–175.
[93] Y. Ling, J. Rubin, Y. Deng, C. Huang, U. Demirci, J.M. Karp, A. Khademhosseini, A cell-laden microfluidic hydrogel, Lab Chip 7 (6) (2007) 756–762.
[94] A.P. Golden, J. Tien, Fabrication of microfluidic hydrogels using molded gelatin as a sacrificial element, Lab Chip 7 (6) (2007) 720–725.
[95] W. Lee, V. Lee, S. Polio, P. Keegan, J.H. Lee, K. Fischer, J.K. Park, S.S. Yoo, On-demand three-dimensional freeform fabrication of multi-layered hydrogel scaffold with fluidic channels, Biotechnol. Bioeng. 105 (6) (2010) 1178–1186.
[96] S.H. Lee, J.J. Moon, J.L. West, Three-dimensional micropatterning of bioactive hydrogels via two-photon laser scanning photolithography for guided 3D cell migration, Biomaterials 29 (20) (2008) 2962–2968.
[97] O. Sarig-Nadir, N. Livnat, R. Zajdman, S. Shoham, D. Seliktar, Laser photoablation of guidance microchannels into hydrogels directs cell growth in three dimensions, Biophys. J. 96 (11) (2009) 4743–4752.
[98] U. Watanabe, S. Sugiura, M. Kakehata, F. Yanagawa, T. Takagi, S. Kimio, T. Satoh, M. Tamura, Y. Hosokawa, K. Torizuka, T. Kanamori, Fabrication of hollow structures in photodegradable hydrogels using a multi-photon excitation process for blood vessel tissue engineering, Micromachines (Basel) 11 (7) (2020) 679.
[99] M. Shin, K. Matsuda, O. Ishii, H. Terai, M.R. Kaazempur-Mofrad, J. Borenstein, M. Detmar, J.P. Vacanti, Endothelialized networks with a vascular geometry in microfabricated poly(dimethyl siloxane), Biomed. Microdevices 6 (4) (2004) 269–278.
[100] J. Wang, C. Bettinger, R. Langer, J. Borenstein, Biodegradable microfluidic scaffolds for tissue engineering from amino alcohol-based poly(ester amide) elastomers, Organogenesis 6 (4) (2010) 212–216.
[101] C. Bettinger, E.J. Weinberg, K.M. Kulig, J. Vacanti, Y. Wang, J. Borenstein, R. Langer, Three-dimensional microfluidic tissue-engineering scaffolds using a flexible biodegradable polymer, Adv. Mater. 18 (2) (2005) 165–169.
[102] C. Fidkowski, M.R. Kaazempur-Mofrad, J. Borenstein, J. Vacanti, R. Langer, Y. Wang, Endothelialized microvasculature based on a biodegradable elastomer, Tissue Eng. 11 (1-2) (2005) 302–309.
[103] N. Brandenberg, M.P. Lutolf, Situ patterning of microfluidic networks in 3D cell-laden hydrogels, Adv. Mater. 28 (34) (2016) 7450–7456.
[104] K.A. Heintz, M.E. Bregenzer, J.L. Mantle, K.H. Lee, J.L. West, J.H. Slater, Fabrication of three-dimensional biomimetic microfluidic networks in hydrogels, in: Adv. Healthc. Mater., 5, 2016, pp. 2153–2160.
[105] M.B. Applegate, J. Coburn, B.P. Partlow, J.E. Moreau, J.P. Mondia, B. Marelli, D.L. Kaplan, F.G. Omenetto, Laser-based three-dimensional multiscale micropatterning of biocompatible hydrogels for customized tissue engineering scaffolds, PNAS 112 (39) (2015) 12052–12057.
[106] B. Kang, J. Shin, H.-J. Park, C. Rhyou, D. Kang, S.-J. Lee, Y.-S. Yoon, S.-W. Cho, H. Lee, High-resolution acoustophoretic 3D cell patterning to construct functional collateral cylindroids for ischemia therapy, Nat. Commun. 9 (2018) 5402.
[107] D. Petta, V. Basoli, D. Pellicciotta, R. Tognato, J.P. Barcik, C. Arrigoni, E.Della Bella, A.R. Armiento, C. Candrian, G.R. Richards, M. Alini, M. Moretti, D. Eglin, T. Serra, Sound-induced morphogenesis of multicellular systems for rapid orchestration of vascular networks, Biofabrication (2020) Epub ahead of print.
[108] C.K. Arakawa, B.A. Badeau, Y. Zheng, C.A. DeForest, Multicellular vascularized engineered tissues through user-programmable biomaterial photodegradation, Adv. Mater. 39 (37) (2017) 10.1002/adma.201703156.
[109] V.K. Lee, A.M. Lanzi, N. Haygan, S.S. Yoo, P.A. Vincent, G. Dai, Generation of multi-scale vascular network system within 3D hydrogel using 3D bio-printing technology, Cell. Mol. Bioeng. 7 (3) (2014) 460–472.
[110] X. Wang, D.T.T. Phan, S.C. George, C.C.W. Hughes, A.P. Lee, Engineering anastomosis between living capillary networks and endothelial cell-lined microfluidic channels, Lab Chip 16 (2) (2016) 282–290.
[111] A.A. Szklanny, M. Machour, I. Redenki, V. Chochola, I. Goldfracht, B. Kaplan, M. Epshtein, H.S. Yameen, U. Merdler, A. Feinberg, D. Seliktar, N. Korin, J. Jaroš, S. Levenberg, 3D bioprinting of engineered tissue flaps with hierarchical vessel networks (VesselNet) for direct host-to-implant perfusion, Adv. Mater. 33 (42) (2021) 210661.
[112] J. Son, S.J. Hong, J.W. Lim, W. Jeong, J.H. Jeong, H.-W. Kang, Engineering tissue-specific, multiscale microvasculature with a capillary network for prevascularized tissue, Small Methods 5 (10) (2021) 2100632.
[113] X. Liu, X. Wang, L. Zhang, L. Sun, H. Wang, H. Zhao, Z. Zhang, W. Liu, X. Zheng, Q. Gu, 3D liver tissue model with branched vascular networks bymultimaterial bioprinting, Adv. Healthc. Mater. 10 (23) (2021) 2101405.
[114] P. Orrchetta, R. Visone, L. Russo, L. Cipolla, M. Moretti, M. Rasponi, VA-086 methacrylate gelatine photopolymerizable hydrogels: A parametric study for highly biocompatible 3D cell embedding, J. Biomed. Mater. Res. A 103 (6) (2015) 2109–2117.
[115] A.A. El-Rashidy, S.E. Moshy, I.A. Radwan, D. Rady, M.M.S. Abbass, C.E. Dörfer, K.M.F. El-Sayed, Effect of polymeric matrix stiffness on osteogenic differentiation of mesenchymal stem/progenitor cells: concise review, Polymers (Basel) 13 (17) (2021) 2950.
[116] J. Gu, Q. Zhang, M. Geng, W. Wang, J. Yang, A.U.R. Khan, H. Du, Z. Sha, X. Zhou, C. He, Construction of nanofibrous scaffolds with interconnected perfusable microchannel networks for engineering of vascularized bone tissue, Bioact Mater 6 (10) (2021) 3254–3268.
[117] S. Yin, W. Zhang, Z. Zhang, X. Jiang, Recent advances in scaffold design and material for vascularized tissue-engineered bone regeneration, Adv. Healthc. Mater. 8 (10) (2019) 1801433.
[118] Y. Zheng, Y. Wang, R.K. Chen, S. Deshpande, N.S. Nelson, S.R. Buchman, A.J. Shih, Tissue transformation mold design and stereolithography fabrication, Rapid. Prototyp. J. 23 (1) (2017) 162–168.
[119] G. Turnbull, J. Clarke, F. Picard, P. Riches, L. Jia, F. Han, B. Li, W. Shu, 3D bioactive composite scaffolds for bone tissue engineering, Bioact. Mater. 3 (3) (2017) 278–314.
[120] T. Ahlfeld, A. Lode, R.F. Richter, W. Pradel, A. Franke, M. Rauner, B. Stadlinger, G. Lauer, M. Gelinsky, P. Korn, Toward biofabrication of resorbable implants consisting of a calcium phosphate cement and fibrin-a characterization in vitro and in vivo, Int. J. Mol. Sci. 22 (3) (2021) 1218.
[121] J.B. Vella, R.P. Trombetta, M.D. Hoffman, J. Inzana, H. Awad, D.S.W. Benoit, Three dimensional printed calcium phosphate and poly(caprolactone) composites with improved mechanical properties and preserved microstructure, J. Biomed. Mater. Res. A 106 (3) (2018) 663–672.
[122] B. Zhang, H. Sun, L. Wu, L. Ma, F. Xing, Q. Kong, Y. Fan, C. Zhou, X. Zhang, 3D printing of calcium phosphate bioceramic with tailored biodegradation rate for skull bone tissue reconstruction, Bio-Design Manuf. 2 (3) (2019) 161–171.
[123] J. Filipowska, K.A. Tomaszewki, L. Niedźwiedzki, J.A. Walocha, T. Niedźwiedzki, The role of vasculature in bone development, regeneration and proper systemic functioning, Angiogenesis 20 (3) (2017) 291–302.
[124] M. Loibl, A. Binder, M. Herrmann, F. Duttenhoefer, R.Geoff Richards, M. Nerlich, M. Alini, S. Verrier, Direct cell-cell contact between mesenchymal stem cells and endothelial progenitor cells induces a pericyte-like phenotype in vitro, Biomed. Res. Int. 2014 (2014) 395781.
[125] Y. Liu, S.H. Teoh, M.S. Chong, E.S. Lee, C.N. Mattar, N.K. Randhawa, Z.Y. Zhang, R.J. Medina, R.D. Kamm, N.M. Fisk, M. Choolani, J.K. Chan, Vasculogenic and osteogenesis-enhancing potential of human umbilical cord blood endothelial colony-forming cells, Stem Cells 30 (9) (2012) 1911–1924.
[126] N. Guimarães-Camboa, P. Cattaneo, Y. Sun, T. Moore-Morris, Y. Gu, N.D. Dalton, E. Rockenstein, E. Masliah, K.L. Peterson, W.B. Stallcup, J. CHen, S.M. Evans, Pericytes of multiple organs do not behave as mesenchymal stem cells in vivo, Cell Stem Cell 20 (3) (2017) 345–359.
[127] Q. Ge, H.K. Zhang, J. Hou, L. Wan, W. Cheng, X. Wang, D. Dong, C. Chen, J. Xia, J. Guo, X. Wu, VEGF secreted by mesenchymal stem cells mediates the differentiation of endothelial progenitor cells into endothelial cells via paracrine mechanisms, Mol. Med. Rep. 17 (1) (2018) 1667–1675.
[128] S.M. Bittner, J.L. Guo, A.G. Mikos, Spatiotemporal control of growth factors in three-dimensional printed scaffolds, Bioprinting 12 (2018) e00032.
[129] S. Kuttappan, D. Mathew, J.-I. Jo, R. Tanaka, D. Menon, T. Ishimoto, T. Nakano, S.V. Nair, M.B. Nair, Y. Tabata, Dual release of growth factor from nanocomposite fibrous scaffold promotes vascularisation and bone regeneration in rat critical sized calvarial defect, Acta Biomater. 78 (2018) 36–47.
[130] F.E. Freeman, P. Pitacco, L.H.A. van Dommelen, J. Nulty, D.C. Browe, J.-Y. Shin, E. Alsberg, D.J. Kelly, 3D bioprinting spatiotemporally defined patterns of growth factors to tightly control tissue regeneration, Sci. Adv. 6 (33) (2020) eabb5093.
[131] R.R. Chen, E.A. Silva, W.W. Yuen, D.J. Mooney, Spatio-temporal VEGF and PDGF delivery patterns blood vessel formation and maturation, Pharm. Res. 24 (2) (2007) 258–264.
[132] J.E. Tengood, R. Ridenour, R. Brodsky, A.J. Russell, Sequential delivery of basic fibroblast growth factor and platelet-derived growth factor for angiogenesis, Tissue Eng. Part A 17 (9-10) (2011) 1181–1189.
[133] X. Dong, X. Lu, K. Kingston, E. Brewer, B.A. Julia, O.D. Kripfgans, J.B. Fowlkes, R.T. Franceschi, A.J. Putnam, Z. Liu, M.L. Fabiilli, Controlled delivery of basic fibroblast growth factor (bFGF) using acoustic droplet vaporization stimulates endothelial network formation, Acta Biomater. 97 (2019) 409–419.
[134] T. Gonzalez-Fernandez, S. Rathan, C. Hobbs, P. Pitacco, F.E. Freeman, G.M. Cunniffe, N.J. Dunne, H.O. McCarthy, V. Nicolosi, F.J. O'Brien, D.J. Kelly, Pore-forming bioinks to enable spatio-temporally defined gene delivery in bioprinted tissues, J. Control Release 301 (2019) 13–27.
[135] D.N. Heo, B. Ayan, M. Dey, D. Banerjee, H. Wee, G.S. Lewis, I.T. Ozbolat, Aspiration-assisted bioprinting of co-cultured osteogenic spheroids for bone tissue engineering, Biofabrication (2020) Epub ahead of print.
[136] J. Nulty, R. Burdis, D.J. Kelly, Biofabrication of prevascularised hypertrophic cartilage microtissues for bone tissue engineering, Front. Bioeng. Biotechnol. 9 (2021) 661989.
[137] F.E. Freeman, A.B. Allen, H.Y. Stevens, R.E. Guldberg, L.M. McNamara, Effects of in vitro endochondral priming and pre-vascularisation of human MSC cellular aggregates in vivo, Stem Cell Res. Ther. 6 (2015) 218.
[138] F.E. Freeman, H.Y. Stevens, P. Owens, R.E. Guldberg, L.M. McNamara, Osteogenic differentiation of mesenchymal stem cells by mimicking the cellular niche of the endochondral template, Tissue Eng. Part A 22 (19-20) (2016) 1176–1190.

[139] A. Longoni, I. Pennings, M.C. Lopera, M.H.P. van Rijen, V. Peperzak, A.J.W.P. Rosenberg, R. Levato, D. Gawlitta, Endochondral bone regeneration by non-autologous mesenchymal stem cells, Front. Bioeng. Biotechnol. 8 (2020) 651.
[140] A. Longoni, L. Utomo, A. Robinson, R. Levato, A.J.W.P. Rosenberg, D. Gawlitta, Acceleration of bone regeneration induced by a soft-callus mimetic material, Adv. Sci. (Weinh) 9 (6) (2022).
[141] M. Castilho, M. de Ruijter, S. Beirne, C.C. Viletter, K. Ito, G.G. Wallace, J. Malda, Multitechnology biofabrication: a new approach for the manufacturing of functional tissue structures? Trends Biotech. 38 (12) (2020) 1316–1328.
[142] L. Gutzweiler, S. Kartmann, K. Troendle, L. Benning, G. Finkenzeller, R. Zengerle, P. Koltay, G.B. Stark, S. Zimmermann, Large scale production and controlled deposition of single HUVEC spheroids for bioprinting applications, Biofabrication 9 (2) (2017) 025027.
[143] K. Tröndle, F. Koch, G. Finkenzeller, G.B. Stark, R. Zengerle, P. Koltay, S. Zimmermann, Bioprinting of high cell-density constructs leads to controlled lumen formation with self-assembly of endothelial cells, J. Tissue Eng. Regen. Med 13 (10) (2019) 1883–1895.
[144] P. Rukavina, F. Koch, M. Wehrle, K. Tröndle, G.B. Stark, P. Koltay, S. Zimmermann, R. Zengerle, F. Lampert, S. Strassburg, G. Finkenzeller, F. Simunovic, In vivo evaluation of bioprinted prevascularized bone tissue, Biotechnol. Bioeng. 117 (12) (2020) 3902–3911.
[145] M. de Ruijter, A. Ribeiro, I. Dokter, M. Castilho, J. Malda, Simultaneous micropatterning of fibrous meshes and bioinks for the fabrication of living tissue constructs, Adv. Healthc. Mater. 8 (7) (2019) e1800418.
[146] P.N. Bernal, P. Delrot, D. Loterie, Y. Li, J. Malda, C. Moser, R. Levato, Volumetric bioprinting of complex living-tissue constructs within seconds, Adv. Mater. 31 (42) (2019) e1904209.
[147] D. Loterie, P. Delrot, C. Moser, High-resolution tomographic volumetric additive manufacturing, Nat. Commun. 11 (2020) 852 (2020).
[148] P.N. Bernal, M. Bouwmeester, J. Madrid-Wolff, M. Falandt, S. Florczak, N.G. Rodriguez, Y. Li, G. Größbacher, R.-A. Samson, M. van Wolferen, L.J.W. van der Laan, P. Delrot, D. Loterie, J. Malda, C. Moser, B. Spee, R. Levato, Volumetric bioprinting of organoids and optically tuned hydrogels to build liver-like metabolic biofactories, Adv. Mater. (2022) 2110054.
[149] R. Rizzo, D. Ruetsche, H. Liu, M. Zenobi-Wong, Optimized photoclick (Bio)resins for fast volumetric, Adv. Mater. 33 (49) (2021) 2102900.